https://doi.org/10.1016/j.apenergy.2021.118213

A proposed paper submitted to
Applied Energy

Numerical and experimental investigations on thermal management for data center with cold aisle containment configuration

Yee-Ting Lee [a,b], Chih-Yung Wen [c], Yang-Cheng Shih [a,b], Zhengtong Li [c] and An-Shik Yang [a,b] *

[a] Department of Energy and Refrigerating Air-Conditioning Engineering, National Taipei University of Technology, Taipei 106, Taiwan
[b] Research Center of Energy Conservation for New Generation of Residential, Commercial, and Industrial Sectors, National Taipei University of Technology, Taipei 106, Taiwan
[c] Department of Mechanical Engineering, The Hong Kong Polytechnic University, Kowloon, Hong Kong

Mailing Address:
Dr. An-Shik Yang (*Corresponding Author)
Distinguished Professor and Department Chairman
Department of Energy and Refrigerating Air-Conditioning Engineering
National Taipei University of Technology
1, Sec. 3, Chung-Hsiao E. Rd., Taipei 106, Taiwan
Tel: (886) 2-2771-2171 ext. 3523
Fax: (886)2-2731-4919
Email: asyang@ntut.edu.tw

Keywords: Data center, Airflow management, Rack cooling index, Return temperature index, Supply heat index, CFD simulation

The short version of the paper (Ref. No. ICAE-61) was presented at ICAE2020, Dec. 1-Dec. 10, Bangkok/Virtual. This paper is a substantial extension of the short version of the conference paper.

Abstract

This study proposes the container data center with the featured cold aisle containment (CAC) as effective thermal control strategy. In design, the overhead downward flow system is implemented with a heat exchanger arranged right above the data center on the air side and an evaporative water chiller on the water side to form the cooling approach. The cold airflows and hot exhausts of racks are separately transported by the contained cold and hot aisles to alleviate the problem of cold and hot air mixing. The measurements of air temperature and velocity of racks are used to validate the prediction accuracy of the computational fluid dynamics (CFD) model. The performance metrics in terms of the rack cooling index (RCI), return temperature index (RTI), supply heat index (SHI) are used to examine the design effectiveness of the proposed test data center. The simulations are then extended to assess the air distribution and thermal management at varied supply air temperatures and velocities for a large-scale data center to be built in the green energy technology demonstration site of the Shalun smart green energy science city. Overall, the calculated average PUE of 1.38 for the large-scale data center is notably less than the average PUE of 1.59 from the results of 2020 data center industry survey, indicating the potential savings of cooling energy and cost. This paper demonstrates a generalized approach as an easily adaptable, cost-effective solution for data centers to be deployed in tropical and subtropical areas.

Keywords: Data center, Airflow management, Rack cooling index, Return temperature index, Supply heat index, CFD simulation

1. Introduction

In recent years, new technologies such as cloud computing, artificial intelligence (AI), fifth generation (5G) communication, and internet of things (IoT) have substantially changed the way of people to live, work, connect and learn in every aspect with the rapid development of globalization and informationization [1]. The related information processes are normally fulfilled in a so-called data center, which is a particular facility housing multiple network segments for data computing, processing, storing and sharing sequences. Having great processing capability, the centralized data centers also consume enormous power. For instance, data centers in the United State are anticipated to consume nearly 0.073 PWh in 2020, corresponding to a yearly increase rate of 4% between 2014 and 2020 [2]. According to the report from Lawrence Berkeley National Laboratory (LBNL) [3], data centers in US expended approximate 70 TWh electricity in 2016, accounting for 1.8% of the annual electricity generation. Based on the current trend, the power consumption of global data centers is presumed to use about one-fifth of the entire world's electricity by 2025 [4]. Among the total energy consumption, the cooling system is conventionally responsible for 40–60% in average to ensure the sustainable and reliable operations of equipment [5]. In consideration of reducing the operating cost, the improvement of cooling efficiency of data center can mitigate power demand.

Data centers can be fifty times more power-intensive than commercial buildings in operations

The short version of the paper (Ref. No. ICAE-61) was presented at ICAE2020, Dec. 1-Dec. 10, Bangkok/Virtual. This paper is a substantial extension of the short version of the conference paper.

[6]. During the last decade, substantial advances have been completed by associate organizations to pinpoint the major difficulties of data center efficiency. Therefore, the endeavors of developing standards and identifying best practices are exploited to achieve enhancement of energy efficiency. Introduced by the Green Grid initiative as a widely used indicator of data center energy efficiency, the power usage effectiveness (PUE) is defined as the ratio of the total power needed for system operations (including the cooling, power distribution and other overheads) to the power consumed only by the equipment of information technology (IT) [7]. The nominal PUE value for the type of green data center is less than 1.5, whereas PUE of 1.2–1.3 can be commonly considered as energy optimization of data centers [8]. In practice, PUE can be varied relating to the weather situations and geographical regions. Although data centers with the outdoor cold air totally applied to the cooling unit tend to lessen PUEs [9], it can be inevitable to locate those data centers in tropical and subtropical climatic areas attributable to the concerns of convenient power source and data/power transmission [10]. However, it remains unfeasible to utilize the outside air for the cooling purposes in hot and humid areas [11]. Therefore, in the modern high power density server environment, the proper arrangement of air distribution is an effective way to enhance energy efficiency of cooling system [12].

In effect, the avoidance of hot and cold air mixing is a key for cost-effective cooling strategies of data centers. The enclosed aisle can adequately resolve this problem to decrease the air inlet temperature of the rack for enhancing the cooling performance [13]. Accordingly, the containment of hot-aisle or cold-aisle all over the data center is a useful approach for thermal management and energy saving. Nada and Elfeky [14] implemented the proposed cold aisle containments into data centers to improve the thermal environments of IT servers. The results demonstrated the notable advance of thermal performance of servers using entirely enclosed cold aisles in data centers. Gondipalli, Bhopte, Sammakia, Iyengar and Schmidt [15] indicated a reduction in the rack inlet temperature up to 40% through isolating the cold aisle without changing the computer room layout and cold air supply. Evaluating the cooling outcomes of an actual data center in Finland for one-year operation, Lu, Lü, Remes and Viljanen [16] achieved 15–25% energy saving through the full separation of airflows from mixing. Khalaj, Scherer, Siriwardana and Halgamuge [17] addressed the solution details in thermal management for data centers. A number of undesirable hot spots near the racks were detected with the form of open aisles. Various thermal evaluation indexes, including the rack cooling index (RCI), supply heat index (SHI), and return temperature index (RTI) have been broadly used to appraise the design effectiveness of system architecture of data centers. Adopting the CAC strategy, the related SHI, RCI and coefficient of performance (COP) of cooling system are improved by more than 0.45, 17% and 19.5%, respectively. Besides, Gao, Yu and Wu [18] compared the cooling performance of the data center with and without the CAC layout by CFD simulations. It was shown that the supplied air temperature could be increased by 3 °C via utilizing the CAC design while still maintaining the thermal ambient within the recommended

The short version of the paper (Ref. No. ICAE-61) was presented at ICAE2020, Dec. 1-Dec. 10, Bangkok/Virtual. This paper is a substantial extension of the short version of the conference paper.

range. The aforementioned findings have pinpointed improved operational efficiency utilizing the design of containment systems in data centers. Nevertheless, the associated ventilation layouts still applied the underfloor air distribution (UFAD) configurations, producing high pressure drops due to long airflow path lengths to cause poor operational performance and excessive energy consumption. The frequent occurrences of hot air recirculation and cold air bypass are known as other drawbacks. In contrast, the overhead downward flow approach employing the gravity assistance of cold air can smoothly distribute the airflows into each rack. Schmidt, Iyengar, Vogel and Pienta [19] also reported better thermal performance of the overhead down flow system at the inlet of the racks than the UFAD system under certain circumstances. Moreover, the implementation of heat exchangers at the top of racks on the air side can cool the ascending hot exhausts from the hot aisle, avoiding the heated air traveling through a long distance to CRACs for inefficient operations of cooling equipment. Meanwhile, the unevenness of air supply can be lessened to prevent the mixing of cold and hot airflows in recirculation areas due to the formation of hot spots in the cold aisle. Then again, energy efficient cooling is critical to constructing more endurable data center operations.

Additionally, free cooling with water is an economic and environmentally friendly alternative to producing cold. The exploitation of natural cold energy to replace or assist mechanical cooling by Han, Zhang, Meng, Liu, Li and Han et al. [20], Harby, Gebaly, Koura and Hassan [21] and Han, Ji, Wei, Xue, Sun and Zhang et al. [22] can even further achieve maximum energy saving in data centers, as the implementation of free cooling for many countries around the world, the practices performed in the Google data centers can be the well-known example to power cloud communications and networking with less mechanical cooling needed [23]. Hence, data centers can be properly cooled simply by free cooling in particular (cold) regions. However, it can be technically unmanageable to profusely utilize natural cooling sources in those tropical and subtropical areas owing to the lack of low temperature sources, requiring the supportive cooling components integrated with compression refrigeration systems. In this context, previous investigators improved the vapor compressor of air-conditioning system on the air side, such as integrating evaporative cooling air-conditioning system with heat pipes [20], integrated air conditioner with thermosiphon [24], air conditioner with latent heat storage units [25], heat pipes [26], pulsating heat pipe [27], heat pipe with compressor system [28], computer room air handler with direct air-side economizer and computer room air handler with indirect air-side economizer [29] and/or the water side, namely integrated air conditioner with thermosiphon [30], chiller with thermal energy storage system [31], chiller and cooling tower with lake water [32], evaporative condenser [33] and pump-driven loop heat pipe system [34] to reduce energy consumption of cooling equipment. Table 1 presents an extensive overview of the featured cooling systems of data centers. Compared with the existing traditional air conditioners, those enhanced designs demonstrate better energy-saving outcomes for data centers. Specifically, the studies of Han, Ji, Wei, Xue, Sun and Zhang et al. [22], Han, Sun, Wei, Ji and Xue [28] and Liu, Yang, Li and Zhao

The short version of the paper (Ref. No. ICAE-61) was presented at ICAE2020, Dec. 1-Dec. 10, Bangkok/Virtual. This paper is a substantial extension of the short version of the conference paper.

[33] applied the air-conditioning systems with the evaporative water chillers or evaporative condensers on the water side to push the limit temperature of natural cold source to the wet bulb temperature of ambient states for upgrading system performance. The measurement report of testing the performance of evaporative condensers also indicated an increase in system COP results by 11.1% to 29.4.6% compared with the air cooling layout [35]. Therefore, evaporative water chillers adopting the advanced design of impinged sprays with the uniform liquid film dispersion on the water side are applied to increase the exploitation of available natural cold sources for achieving energy savings [36].

In the development of the system having the advantages of efficient cooling and energy saving under variable climate conditions, this study proposes the new close-coupled thermal approach combining a centrifugal fans and a heat exchanger (HX) on the air side and an evaporative water chiller (EWC) on the water side to reduce both the pressure loss of fans and installation space for achieving a compact solution with minimizing the traditional mechanical cooling need. The overhead air delivery technique essentially places the heat exchanger right above the cold aisle. In this manner, the cold air can be supplied directly to the racks by cold aisle containment instead of the entire room, with the hot exhausts of racks absorbed from a contained hot aisle. Accordingly, the problem of cold and hot air mixing is substantially alleviated. This paper experimentally and numerically investigates the operating performance of a simulated container data center with a completely contained cold aisle containment configuration. To validate the numerical model, the computational fluid dynamics (CFD) software ANSYS/Fluent® is applied to predict the velocity and temperature fields around the entry and exit regions of racks in comparison with the experimental results at the inlet velocity of 2.54 m/s and temperature of 291 K. Measures are taken to evaluate the overall performance in terms of the rack cooling index (RCI), return temperature index (RTI) and supply heat index (SHI). CFD calculations are then extended to investigate the influences of the inlet air velocity, inlet temperature and climate conditions on PUE of data centers in the thermal environments located in Shalun (a subtropical city in southern Taiwan). The obtained results can serve as a valuable reference guide and data support for further energy saving analysis. The major contribution of this study is to replace CRAC with the presented design initiative for realizing energy conservation, developing the primary features of next generation data centers. To our best knowledge, similar study has never been reported or discussed in open literature before.

Table 1 Extensive overview of featured cooling systems for data centers

Authors	System descriptions	Reported findings
Okazaki and Seshimo (2011) [24]	Air side: IACT Water side: CT with CH	The operating ratio of compressor for AC system was decreased by approximately 70%.
Sun, Zhang, Medina and Liao	Air side: AC with LHSU Water side: CT with CH	Since only one system operated at a time, the LSHU permitted

The short version of the paper (Ref. No. ICAE-61) was presented at ICAE2020, Dec. 1-Dec. 10, Bangkok/Virtual. This paper is a substantial extension of the short version of the conference paper.

(2015) [25]		substantially shorter running times of the conventional AC. That is, on average the conventional AC ran during 17.4% of the time. The largest ESR of this unit was up to 67% with an average value of 50%.
Tian, He and Li (2015) [26]	Air side: HP Water side: CT with CH	The combined water loop indicated better energy efficiency, with annual cooling power consumption reduced by about 13%. The annual cooling cost was reduced by about 46%.
Zhang, Shao, Xu, Zou and Tian (2015) [30]	Air side: HX Water side: IACT	The EER of thermosyphon mode reached 10.7 and 20.8 when the indoor and outdoor temperature differences were 10 °C and 20 °C, respectively, and the AEER of the IACT was 12.6, which was much higher than traditional AC. The annual energy saving rate was 5.4%–47.3% in four representative climate zones of China.
Lu and Jia (2016) [27]	Air side: PHP Water side: CH	Temperature of the local hotspot was reduced by 3.8 ℃, achieving much uniform temperature distribution.
Oro, Codina and Salom (2016) [31]	Air side: CRAH Water side: CH with TESS	Providing cold energy for 15 min and reducing the scale of UPS; the annual electrical cost was therefore decreased by 3%.
Ling, Zhang, Yu, Ma and Liao (2018) [32]	Air side: CRAH Water side: CH and CT and Lake water	The proposed design could minimize the chiller cooling capacity, and save electricity and cost.
Liu, Yang, Li and Zhao (2018) [33]	Air side: TPCT Water side: EC	The average annual COP of the ideal hybrid refrigeration system was 33, leading to the annual energy savings of nearly 90% compared with the vapor compression refrigeration.
Feng, Li, Zhu, Zhou, Ma and Liu (2018) [34]	Air side: AC Water side: PLHPS	The PLHP system provided the indoor temperature at 18°C to 25°C. About 74.2% of Chinese cities lay in the regions appropriate for applications, and the annual energy saving ratio was over 30%. The average payback period for most cities in China was about3.9 years.

The short version of the paper (Ref. No. ICAE-61) was presented at ICAE2020, Dec. 1-Dec. 10, Bangkok/Virtual. This paper is a substantial extension of the short version of the conference paper.

Han, Ji, Wei, Xue, Sun and Zhang (2020) [22]	Air side: HP with COMPS Water side: EC	The energy consumption was reduced by 31.31%. The COP was increased by 29.49%.
Han, Sun, Wei, Ji and Xue (2021) [28]	Air side: HP with COMPS Water side: EC	PUE reached 1.41, with APF increased by 2.26% to 6.44%.
Jahangir, Mokhtari and Mousavi (2021) [29]	Air side: CRAH with DASE, CRAH with IASE Water side: CH and CT	Using a direct air economizer as the primary cooling system can result in 47% cooling energy saving with 38% NPC reduction. In contrast, the case of using an indirect air economizer can lead to 44% cooling energy saving with 41% NPC reduction throughout 20 years.

AC: Air conditioners; AEER: Annual energy efficiency ratio; APF: Annual performance factor; CH: Chiller; COP: Coefficient of performance; CRAC: Computer room air conditioning; CRAH: Computer room air handler; COMPS: Compressor system; CT: Cooling tower; DASE: Direct air-side economizer; EC: Evaporative condenser; EER: Energy efficiency ratio; ESR: Energy savings ratio; HP: Heat pipe; HX: Heat exchanger; IASE: Indirect air-side economizer; IACT: Integrated air conditioner with thermosiphon; LHSU: Latent heat storage unit; NPC: Net positive cost; PHP: Pulsating heat pipe; PLHPS: Pump-driven loop heat pipe system; TPCT: Two phase closed thermosyphon; TESS: Thermal energy storage system; UPS: Uninterruptible power supply; PUE: Power usage effectiveness.

2. Experimental apparatus

Figure 1 exhibits the schematic diagrams of the cooling and supply air-conditioning systems in the proposed test data center. The present experimental setup implements the overhead downward flow approach with the heat exchanger positioned right above the data center on the air side and an evaporative water chiller on the water side to form the cooling architecture (in Fig. 1). In this proposed design, an evaporative water chiller (JEW-15F/Jesan, Pulse-Luxe, Taiwan) is used as the system refrigeration device to generate the cooling water. In processes, a commercial water pump (YT×2", Yongda Pumping, Taiwan) is operated to transport the cold water from a water buffer tank (with a capacity of 2000 liters) for regulating the water temperature entering the HX. Heat transfer is then achieved with the hot air returning from the hot aisle inside the HX of overhead downward flows. Driven by a centrifugal fan, the cold air runs into the cold aisle, and then diffuses through the racks for taking the server heat away. The associated hot air leaves the racks with heat carried, and returns to the overhead downward flow system via two air-returning ports the ceiling of the test data center. In the end, the heated cold water restores to the chiller for sustaining the purposes of continuous recirculation.

The short version of the paper (Ref. No. ICAE-61) was presented at ICAE2020, Dec. 1-Dec. 10, Bangkok/Virtual. This paper is a substantial extension of the short version of the conference paper.

To analyze the influential parameters of the HX cooling system with the CAC design on the operational performance, an instrumented test data center platform has been constructed to conduct the experiments under various working conditions. The measured data can be then compared with the predicted results to verify the reliability and accuracy of the simulation model. The entire data center is mainly made up of a heat load module (comprising the racks and simulated servers) and a cooling system (involving a HX module and cold air passage). Figure 2 demonstrates the schematic diagram and geometric details of the simulated test data center. The associated dimensions are 2.70 m long × 24.0 m wide × 2.66 m high, respectively. Four standard racks with 1.1-m in length, 0.6-m in width, and 2-m in height are disposed in one row and numbered from A to D correspondingly. Each data rack holds five cabinet layers labeled as server1 to server 5. The cold and hot aisles are positioned in the front and rear of racks, whereas the widths of cold and hot aisles are 1.0 m and 0.6 m, respectively. There are two HXs of equal size (i.e., 2.2 m (L), 1.2 m (W), and 0.66 m (H) each) installed on the top of data center to entrain hot exhaust and supply cold air, while the air-supply extent of two HXs is 1.0 m × 2.4 m, and each air-return port is square, with a size of 0.39 m^2.

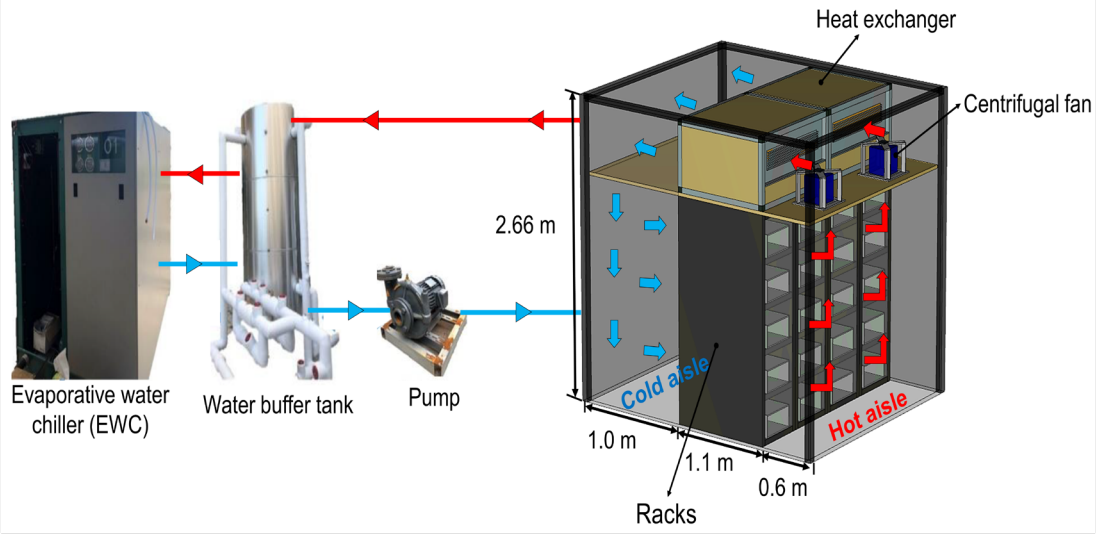

Figure 1 Schematic diagrams of cooling and supply air-conditioning systems in a simulated test data center

The short version of the paper (Ref. No. ICAE-61) was presented at ICAE2020, Dec. 1-Dec. 10, Bangkok/Virtual. This paper is a substantial extension of the short version of the conference paper.

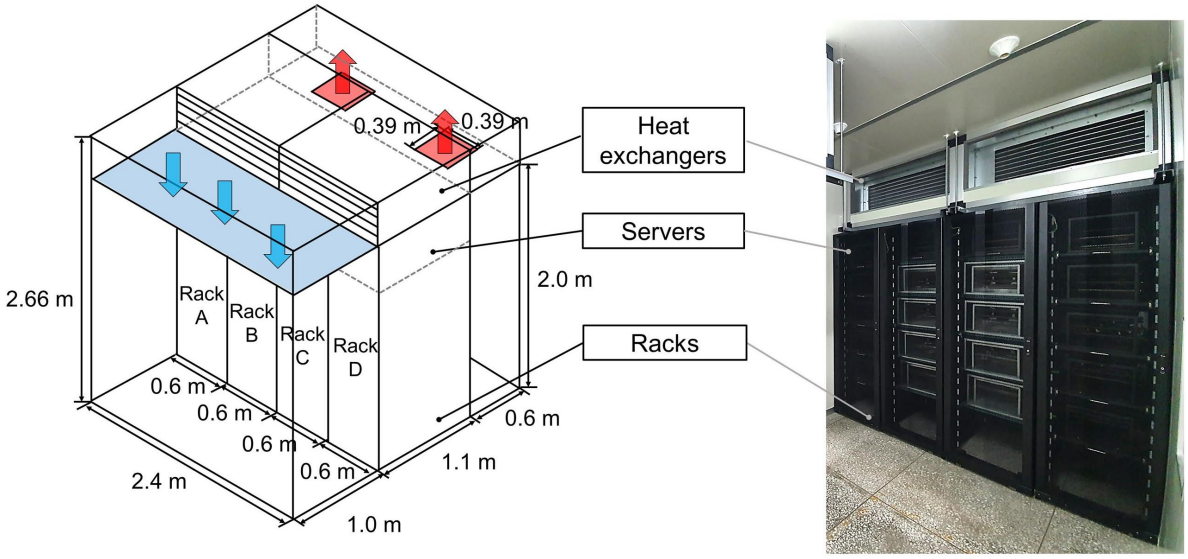

Figure 2 Schematic diagram and relevant geometric details of simulated test data center

This study applies the heaters and fan trays to imitate the thermal behavior of servers. Figure 3 exhibits the schematic diagrams of an individual rack and server. During the test, each rack has five servers. A solid board is used to impede the passage between two servers, as depicted in Fig. 3(a). A 0.5-cm gap between the server and solid board allows the airflow to enter freely. The entrance to each server is made of a grille with perforated holes (in Fig. 3(b)). To imitate the heat generated by the servers, each server places 6 copper tubes as the heater source of 1.8 kW. Accordingly, the associated power density is 9.0 kW per rack, achieving a total power of 36 kW in the tests. Two fans (AGE15051_24J, Delta) are mounted in the downstream area of a server to provide a standard volumetric flowrate of 0.248 m^3/s with a rated speed of 3500 rpm at ambient pressure. Referring to the ASHRAE 41.2 standard [37], the measurements of inlet and outlet air temperatures of the racks are performed without disturbing the flow field. In effect, the inlet and outlet air temperatures of severs are measured employing 10 thermocouple arrays (with 6 rows×4 columns each) installed on the loose metal meshes, including 240 monitoring points in total for five servers. The distance between the rack door and metal mesh is retained below 50 mm. Table 2 shows the specifications of measuring instruments, including the instrument name, model number, measurement range, accuracy and manufacturer for each device. In experiments, the T-type thermocouples are installed in the measured temperatures with an accuracy of ±0.10 °C after calibration. The temperature at a specific position is the averaged value of those thermocouples. The data acquisition system (GM10, Yokogawa) is utilized to record temperatures for every 2.0 s. The airflow velocities through each server are evaluated utilizing a hot-wire anemometer (Testo 0635-1050 and Testo 480, Testo) with a measuring span of 0–10 m/s and an accuracy of ±0.03 m/s + 5% measured value of the reading. This study also employ an adjustable mounting platform to carry out 12 measurements for the inlet or outlet planes of servers. The power meter (PW3360-20, HIOKI) is used to obtain the power use from each component of the cooling and IT systems in the simulated data center. The accuracy for

The short version of the paper (Ref. No. ICAE-61) was presented at ICAE2020, Dec. 1-Dec. 10, Bangkok/Virtual. This paper is a substantial extension of the short version of the conference paper.

the power meter is ± 0.3% of its reading value. Further descriptions on the experimental details can be referred to Chu, Wang, Hsu and Wang [38].

Table 2. Specifications of measuring instruments

Instrument	Model number	Range	Accuracy	Manufacturer
Thermal anemometer	Testo 0635-1050 and Testo 480	0–10 m/s	±0.03 m/s +5% measured value RD	Testo
Temperature sensor	T-type thermocouple	-100 °C–400°C	±0.10 °C	Omega Engineering
Power Meter	PW3360-20	300.00 W–9.0000 MW	±0.3% RD	HIOKI

RD: Reading

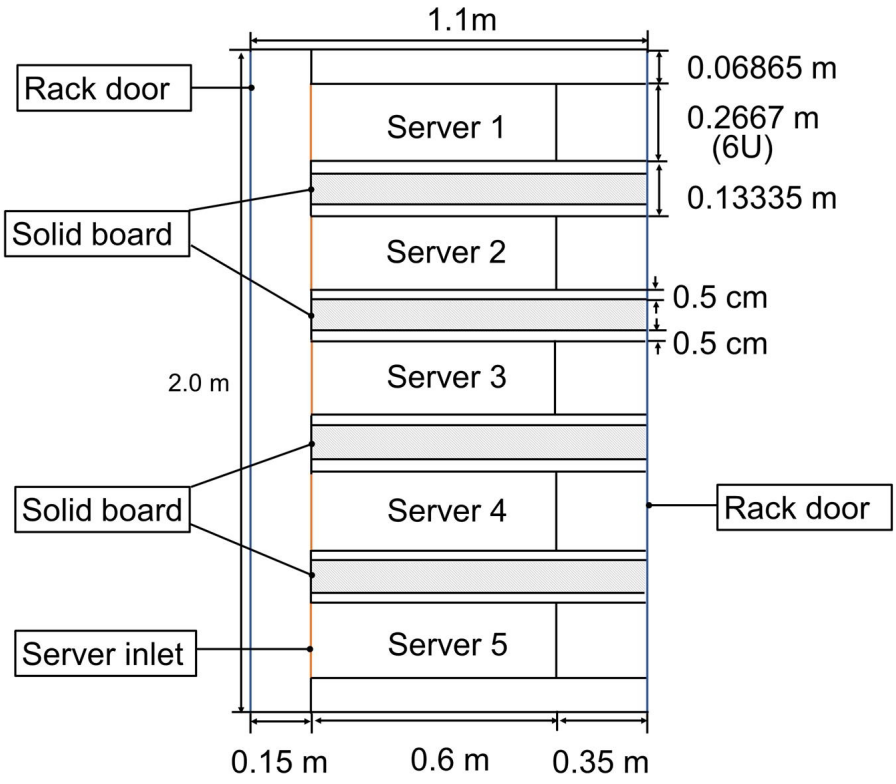

(a)

The short version of the paper (Ref. No. ICAE-61) was presented at ICAE2020, Dec. 1-Dec. 10, Bangkok/Virtual. This paper is a substantial extension of the short version of the conference paper.

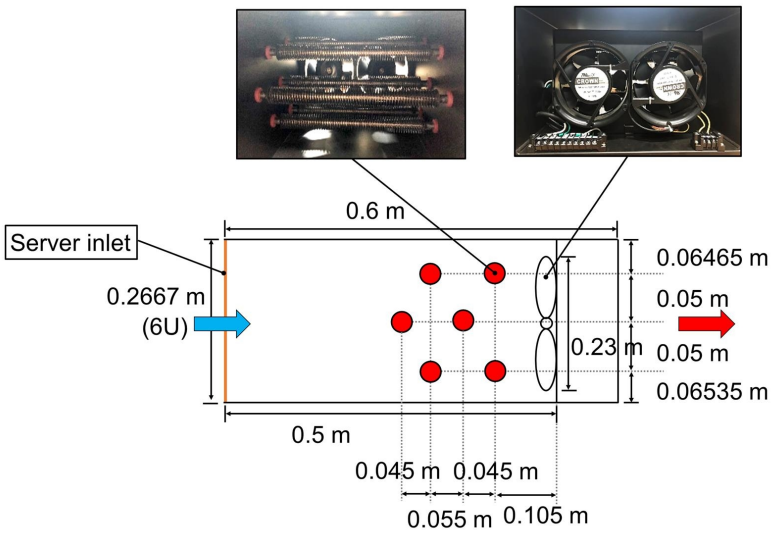

(b)

Figure 3 Schematic diagrams of (a) rack and (b) server in a cross-sectional view

The efficiency and thermal performance of data centers can be evaluated employing the intake temperatures before the server racks, with the equipment intake temperatures corresponding to the thermal environments. There is common practice of performance metrics to quantify the conformity with thermal data center standards such as ASHRAE and NEBS [14]. In this study, the performance measurement index of rack cooling index (RCI) is suitable to evaluate the influences of hot air recirculation on the cooling efficiency in data centers [39]. Exactly, the condition of RCI_{HI}= 100% represents that no intake temperature is above the maximum recommended, and RCI_{LO}= 100% designates that no intake temperature is below the minimum recommended. Both numbers equal to 100% revealing absolute compliance, i.e., all intake temperatures are within the recommended range. Mathematically, the RCI_{HI} and RCI_{LO} are given as:

$$\mathrm{RCI_{HI}} = \left[1 - \frac{\Sigma\left(T_x - T_{\max-rec}\right)_{T_x > T_{\max-rec}}}{\left(T_{\max-all} - T_{\max-rec}\right)n}\right] \times 100\%, \quad (1)$$

$$\mathrm{RCI_{LO}} = \left[1 - \frac{\Sigma\left(T_{\min-rec} - T_x\right)_{T_{\min-rec} > T_x}}{\left(T_{\min-rec} - T_{\min-all}\right)n}\right] \times 100\%. \quad (2)$$

Where T_x denotes the mean intake temperature into the racks, n is the number of computer rack. $T_{max\text{-}rec}$ is the maximum recommended intake temperature (= 27 °C), $T_{max\text{-}all}$ symbolizes the maximum allowable intake temperature (= 32 °C), $T_{min\text{-}rec}$ denotes the minimum recommended intake temperature (= 18 °C), and $T_{min\text{-}all}$ is the minimum allowable intake temperature (= 15 °C) [40]. In this study, the inlet temperatures are within 18 °C to 27 °C; therefore, the corresponding calculated RCI essentially equals to RCI_{LO}.

The performance assessment in terms of the return temperature index (RTI) is appropriate to assess the airflow rate effect on the cooling efficiency in data centers [41]. The RTI is defined as

The short version of the paper (Ref. No. ICAE-61) was presented at ICAE2020, Dec. 1-Dec. 10, Bangkok/Virtual. This paper is a substantial extension of the short version of the conference paper.

the ratio of total airflow through the CRACs (corresponding to the HXs in this case) to the total airflow through the rack. The RTI value above 100% points toward the occurrence of re-circulation and an increase in the air intake temperatures of the rack; on the other hand, the RTI under 100% means the cold airflow by-passing the electronic equipment. The target RTI value is 100% as a measure of the energy performance.

$$\mathrm{RTI} = \left(\frac{T_R - T_s}{\Delta T_{\mathrm{Equip}}} \right) \times 100\% \cdot \tag{3}$$

Here the signs T_R and T_s represent the outlet and inlet temperatures from the HXs. ΔT_{Equip} is the weighted average temperature rise across the equipment [41].

The recirculation of hot air can significantly affect the thermal efficiency of data centers. The dimensionless parameter of supply heat index (SHI) was proposed by Sharma, Bash and Patel [42], denoting the sensible gained heat by air in the cold aisle before entering racks. The SHI is defined as follows:

$$\mathrm{SHI} = \frac{T_{in} - T_{ref}}{T_{out} - T_{ref}} \cdot \tag{4}$$

where T_{in} and T_{out} mean the rack inlet and outlet temperatures. As a reference temperature, T_{ref} is the air temperature from a HX. The SHI may reach zero when no recirculation occurs. An increase in SHI can result in the pronounced outcomes of hot-air recirculation. The cooling system in the data center becomes more susceptible to failure. Accordingly, SHI can be used as an indicator of thermal management and energy efficiency in data centers.

3. Numerical simulation and validation

3.1 Physical model and computational mesh settings

As described in Section 2 Experimental apparatus, this study firstly replicates the geometrical details of simulated test data center from the test setup to generate a three-dimensional (3D) CFD mesh system for code validation (in Fig. 2). CFD calculations are then extended using the validated computational model to complete the facility assessments of airflow and thermal management for a large-scale data center to be constructed in the green energy technology demonstration site of the Shalun smart green energy science city, Tainan, Taiwan. Figure 4 shows the schematic diagram of a large-scale data center in a top view. A physical model for this planned large-scale data center has been built with the dimensions of 11.0 m (L) × 13.1 m (W) × 3.0 m (H), respectively. To apply the cold aisle containment with the HX cooling system, there are 4 primary rows (each with 10 racks), dividing into two cold aisles (marked in blue color), a common hot aisle arranged in the middle and two individual hot aisles on the two sides of data center. The conventional rack size of 1.1 m (L) × 0.6 m (W) × 2.0 m (H) is considered with the rows of racks labeled as A to D in the large-scale data center. This study applies ANSYS Workbench® 19.0 to realize the meshing setup, using the structured hexahedral cells over the computational domain to characterize the airflow distribution

The short version of the paper (Ref. No. ICAE-61) was presented at ICAE2020, Dec. 1-Dec. 10, Bangkok/Virtual. This paper is a substantial extension of the short version of the conference paper.

within the data center. Figure 5 illustrates the computational meshes for the (a) simulated test data center and (b) large-scale data center. To attain the local grid refinement with hexahedral cells over the computational domain for both the models of simulated test data center and large-scale data center, more grids are disposed surrounding the copper tubes (as the heat source) inside the severs as well as the exterior surfaces of the racks to better resolve the underlying rapid variations of air velocity and temperature. Those cells in the vicinity of copper tubes and boundary surfaces implement a peak stretching ratio of 1.1 with the smallest cell volumes of approximately 4.8×10^{-7} m^3 and 9.2×10^{-6} m^3, respectively, corresponding to the y^+ values varied from 26 to 41. In practice, the values of the minimum orthogonal quality, greatest aspect ratio and peak cell skewness are 0.74/0.71, 5.20/5.80 and 0.67/0.72, respectively, suggesting the realization of high- quality meshes. These settings can appropriately locate the wall-adjacent cells over the logarithmic layer to well comply with the requirements of employing the standard wall functions. The total grid numbers of the simulated test data center and large-scale data center are 4,245,462 and 32,070,240, respectively.

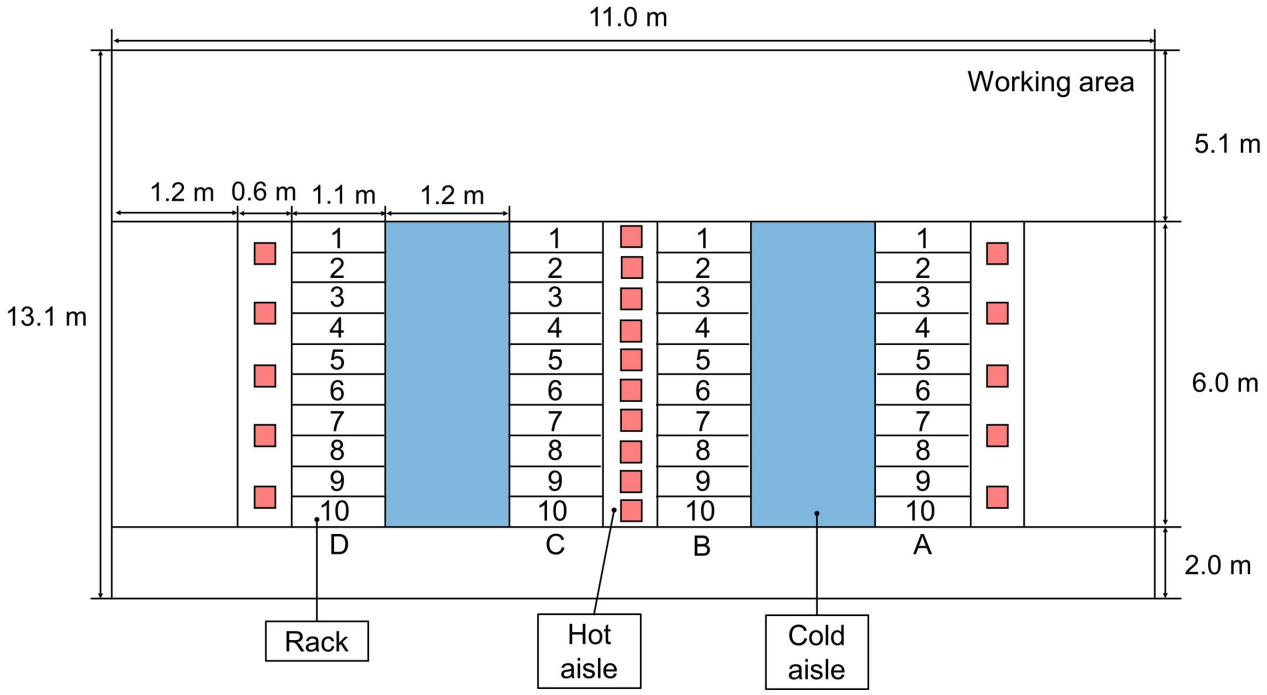

Figure 4 Schematic diagram of large-scale data center in a top view

The short version of the paper (Ref. No. ICAE-61) was presented at ICAE2020, Dec. 1-Dec. 10, Bangkok/Virtual. This paper is a substantial extension of the short version of the conference paper.

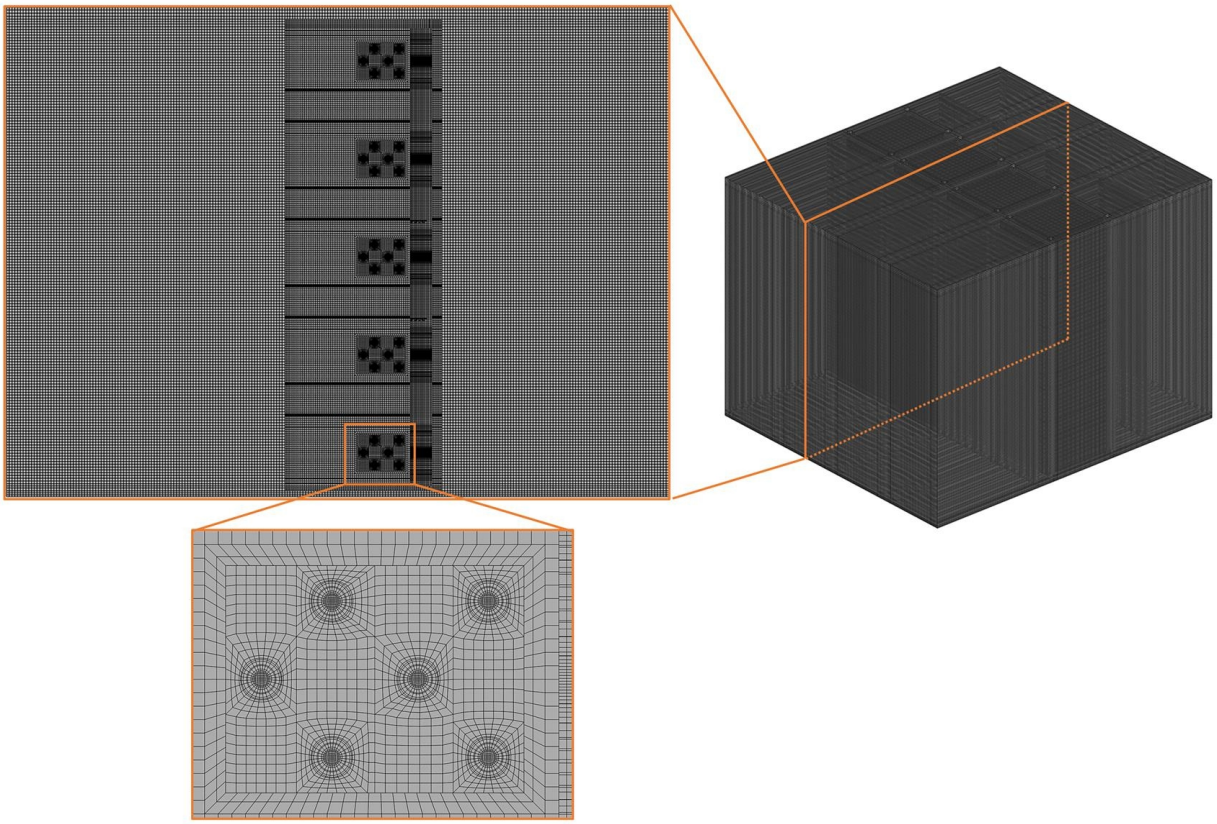

(a)

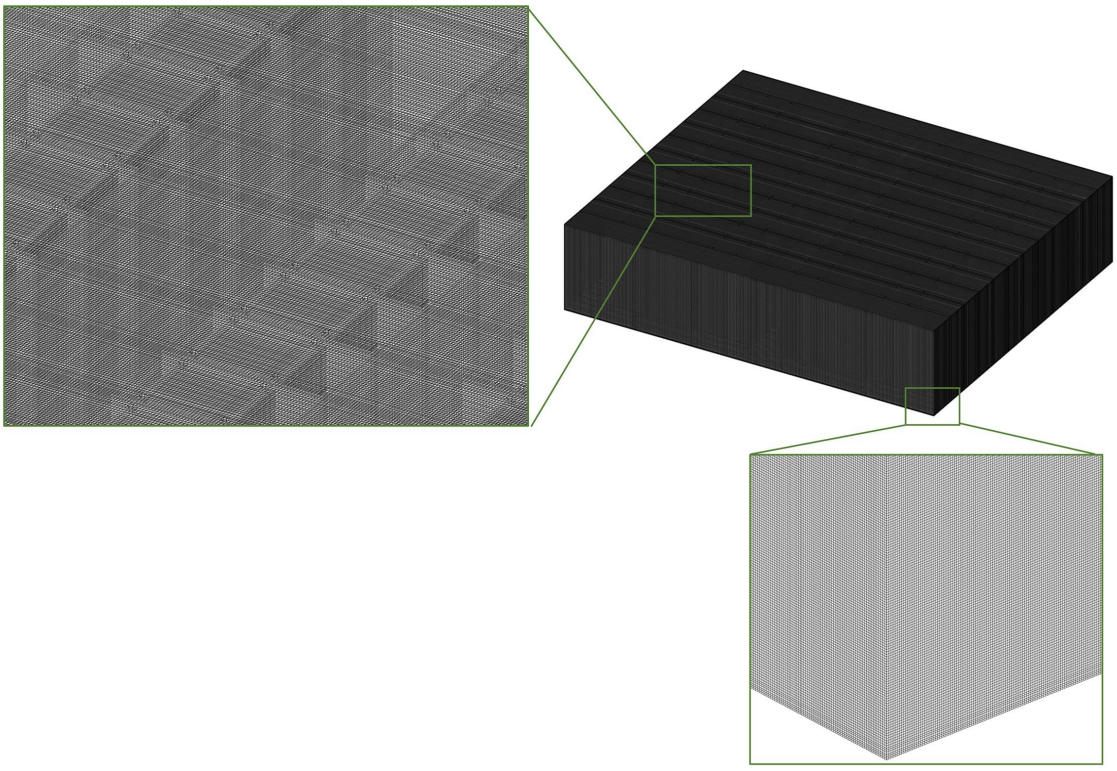

(b)

The short version of the paper (Ref. No. ICAE-61) was presented at ICAE2020, Dec. 1-Dec. 10, Bangkok/Virtual. This paper is a substantial extension of the short version of the conference paper.

Figure 5 Computational meshes for (a) simulated test data center and (b) large-scale data center

3.2 Governing equations and numerical methodology

This study utilizes the commercial CFD software ANSYS/Fluent® to investigate thermo-fluid characteristics of the proposed data centers. In the assumptions made in numerical simulations, the incompressible airflows across data centers are considered neglecting the viscous heat dissipation. Airflows are delivered into the data centers from HXs, and then return to HXs after cooling the rack equipment. The present model treats density as a constant in all equations except for the buoyancy term in the momentum equation. The Boussinesq approximation is therefore applied to simulate the buoyancy force for natural-convection flows. The rack panels and inner partitions of data centers are assumed insulated to simplify the solution process, with negligible heat radiation between each surface in the data centers. Moreover, this study assumes no heat dissipation from the outer surfaces of rack doors, indicating the isolation of data centers from the external environment. The analysis is based upon the finite control volume approach of Reynolds-averaged Navier–Stokes (RANS) and energy equations in conjunction with a realizable *k–ε* turbulence model. The governing equations can be expressed as below.

$$\nabla \cdot \vec{V} = 0\,, \tag{5}$$

$$\rho \vec{V} \cdot \nabla \vec{V} = -\nabla p + \nabla \cdot (\mu_{eff} \nabla \vec{V}) + \rho_{ref}\, \vec{g} \beta \left(T - T_{ref}\right), \tag{6}$$

$$\rho C \vec{V} \cdot \nabla T = \nabla \cdot (\lambda_{eff} \nabla T)\,. \tag{7}$$

Here the signs $\vec{V}$, p, ρ, μ_{eff}, $\vec{g}$, C, T and λ_{eff} denote the velocity vector, pressure, density, effective dynamic viscosity (consisting of the laminar viscosity μ and turbulent viscosity μ_t), gravitational acceleration, specific heat, temperature and effective thermal conductivity, respectively. The model treats density as constant in all equations, except in the buoyancy term of the momentum equation. This study implements the Boussinesq approximation, $\rho = \rho_{ref}\, \beta\, (T - T_{ref})$ in Eq. (6), to model the buoyancy-driven flow, whereas β, T_{ref} and ρ_{ref} signify the thermal expansion coefficient, reference temperature and reference density. Considering the complicated flow nature owing to the elaborate geometries of the data center with the cold aisle containment configuration, the realizable *k-ε* model is employed for turbulence closure to provide superior performance for flows involving the separation, vortices and recirculation as well as the boundary layer flows under strong adverse pressure gradients [43].

$$\nabla\left(\rho k \vec{V}\right) = \nabla \cdot \left(\left(\mu + \frac{\mu_t}{\sigma_k}\right)\nabla k\right) + \mu_t S^2 - \rho\varepsilon\,, \tag{8}$$

$$\nabla\left(\rho \varepsilon \vec{V}\right) = \nabla \cdot \left(\left(\mu + \frac{\mu_t}{\sigma_\varepsilon}\right)\nabla \varepsilon\right) + C_1 S \rho \varepsilon - C_2 \frac{\rho \varepsilon^2}{k + \sqrt{\nu \varepsilon}}\,. \tag{9}$$

The short version of the paper (Ref. No. ICAE-61) was presented at ICAE2020, Dec. 1-Dec. 10, Bangkok/Virtual. This paper is a substantial extension of the short version of the conference paper.

Where the symbols k and ε are the turbulent kinetic energy and turbulent energy dissipation rate, with turbulent viscosity μ_t calculated by $C_\mu \rho k^2/\varepsilon$ (C_μ is a turbulent constant). The variable S equals to $(2S_{ij}S_{ij})^{0.5}$ with $S_{ij}=0.5(\partial u_i/\partial x_j+\partial u_j/\partial xi)$. The factor C_1=max [0.43, $\eta/(\eta+5)$] and $\eta= S(k/\varepsilon)$. The constants C_μ, C_2, σ_k and σ_ε are given as 0.09, 1.9, 1.0 and 1.2, respectively. To avoid the numerical false diffusion and increase the numerical accuracy, the second-order upwind numerical scheme is used to solve the discretized convection-diffusion terms. During the iterative process, an iterative semi-implicit method for pressure-linked equations consistent (SIMPLEC) algorithm is adopted for the pressure-velocity coupling [44]. The values of density, viscosity and conductivity of air are 1.212 kg/m^3, 1.803×10^{-5} N-s/m^2 and 2.572×10^{-2} W/m-k at the rack inlet temperature of 291 K as the baseline case.

In effect, the airflows tend to be rectified throughout the rack door and grille of the server entrance, with the heat generation inside the server evenly carried to the hot aisle. Utilizing the approach of a porous jump, the pressure drops (Pa) to simulate the inlets of racks and servers are expressed as below [45].

$$\Delta P = 2.6V^2, \tag{10}$$

$$\Delta P = 0.4757V^2 + 1.4664V. \tag{11}$$

Here ΔP and V are the pressure drop and velocity magnitude across the grilles (i.e., 0.003 m thick and 0.002 m thick) of the server inlet and rack doors, respectively. Besides, the related P-Q curve of those fans supplied by the manufacturer is given to model the performance of the fans installed in the back of the servers, as follows.

$$\Delta P = 201.309 - 931.389Q^2, \tag{12}$$

where Q is the volume flow rate (m^3/s).

In consistency with the measurements, the vertically downward airflow velocity of 1.53 m/s at 291 K is specified as the inlet boundary condition of the simulated test data center under steady operations. On the other hand, the supply airflow velocity and temperature of the large-scale data center vary from 1.85 m/s to 4.06 m/s and from 291 K to 300 K, respectively. Furthermore, each of five server simulators is set at the heat dissipation of 1.8 kW (9 kW per rack). The exhaust vent is modeled as a pressure outlet with an ambient pressure of 1 atm. All other boundaries are assumed adiabatic.

3.3 Grid independence test and model validation

To conduct the grid-independent studies for both the simulated test data center and large-scale data center, the average hot air return temperatures to the HX within the data center are chosen as the crucial parameter to examine the mesh-convergent condition, as suggested by Lu and Zhang [46] and Gupta, Asgari, Moazamigoodarzi, Pal and Puri [47]. Table 3 illustrates the results of mesh independence on the average hot air return temperatures to HX for both the simulated test data

The short version of the paper (Ref. No. ICAE-61) was presented at ICAE2020, Dec. 1-Dec. 10, Bangkok/Virtual. This paper is a substantial extension of the short version of the conference paper.

center and large-scale data center. In the former case of simulated test data center, three computations are conducted with the total grid numbers of 1,675,588, 4,245,462 and 9,345,415, respectively. The difference by comparing the average hot air return temperatures utilizing 1,675,588 grids with 9,345,415 grids is 0.32%. Further testing indicates a decrease in the variation of predictions to 0.062% for 4,245,462 and 9,345,415 grids, suggesting good grid independence with 4,245,462 grids. In the latter case of large-scale data center, we also accomplish the grid independency study at three mesh levels with the total grids of 12,828,096, 32,070,240 and 70,899,858 points, respectively. The CFD results show the asymptotic tendency of hot air return temperatures toward their stable states for an increase in total number of grids from 12,828,096 to 70,899,858. The discrepancy of hot air return temperatures to the HX is 0.47% using 12,828,096 and 70,899,858 grids. However, the associated difference of calculations reduces to 0.055% for the meshes based on 32,070,240 and 70,899,858 grids, revealing agreeable grid independence attained by 32,070,240 grids for confirming an insignificant effect of mesh setup on the predictions.

Table 3 Mesh independence results on average hot air return temperatures to HX for both the simulated test data center and large-scale data center

Number of cells for simulated test data center	Average hot air return temperatures to HX (K)	Difference (%)
1,675,588	301.32	0.32%
4,245,462	302.11	0.062%
9,345,415	302.30	-
Number of cells for large-scale data center	**Average hot air return temperatures to HX (K)**	**Difference (%)**
12,828,096	302.86	0.47%
32,070,240	303.45	0.055%
70,899,858	303.62	-

To validate the accuracy of CFD predictions, the measurements of inlet air temperature and velocity are conducted and compared with the calculated results. During operations, the conditions of supply air temperature (T_{in}) of 291 K and inlet velocity of 1.53 m/s are adopted for the simulated test data center. In experiments, each data point represents the mean value of 5 to 8 measured data points with the error bars specified by $\pm 3\sigma_{sd}$, where σ_{sd} is the standard deviation. Figure 6 illustrates the comparison between the CFD predictions and experimental measurements of the averaged inlet

The short version of the paper (Ref. No. ICAE-61) was presented at ICAE2020, Dec. 1-Dec. 10, Bangkok/Virtual. This paper is a substantial extension of the short version of the conference paper.

(a) air velocities and (b) air temperatures of severs. Essentially, the overhead downward flow arrangement tends to produce lower inlet air temperatures and higher inlet air velocities on the top parts of all racks, as compared to the bottom parts. The simulations reveal the similar tendency to those measurements of air velocity and temperature (as depicted in Fig. 6(a)). The inconsistencies between the predictions and measured average air velocities for the 5 servers installed into Rack A to Rack D range from 1.12% to 3.30%. Moreover, the differences of calculated inlet temperatures with experimental data vary from 0.06% to 0.59% (in Fig. 6(b)). It can be attributed to the reason of simplification of CFD model having a relatively larger cross-sectional area of the air passage across each server, as compared to that of the actual data center. Accordingly, the predicted air velocities are fairly lower than the experimental data. Alternatively, the measured temperatures are slightly higher than the CFD results. The difference may be caused by the effects of air leakage and heat sources like lights on the temperature, which are not considered in the computational modeling. Similar descriptions are also made in the studies of Lu and Zhang [46], Jin and Bai [48] and Tradat, Sammakia, Hoang and Alissa [49]. The comparison of predictions of performance indices in terms of RCI_{Lo}, RTI and SHI is also in good agreement with the measurements shown in Table 4. For those data centers without utilizing the CAC design (for instance, the scenarios described by Nada and Elfeky [14], Gao, Yu and Wu [18] and Chu, Hsu, Tsui and Wang [50], the poor air distribution and mixing of hot and cold air deteriorate the performance indicators of RCI, RTI and SHI ranging 47% to 80%, 82% to 105% and 0.26 to 0.37, respectively, revealing realization of the smooth distribution of airflows into each rack due to the present overhead downward flow approach.

The short version of the paper (Ref. No. ICAE-61) was presented at ICAE2020, Dec. 1-Dec. 10, Bangkok/Virtual. This paper is a substantial extension of the short version of the conference paper.

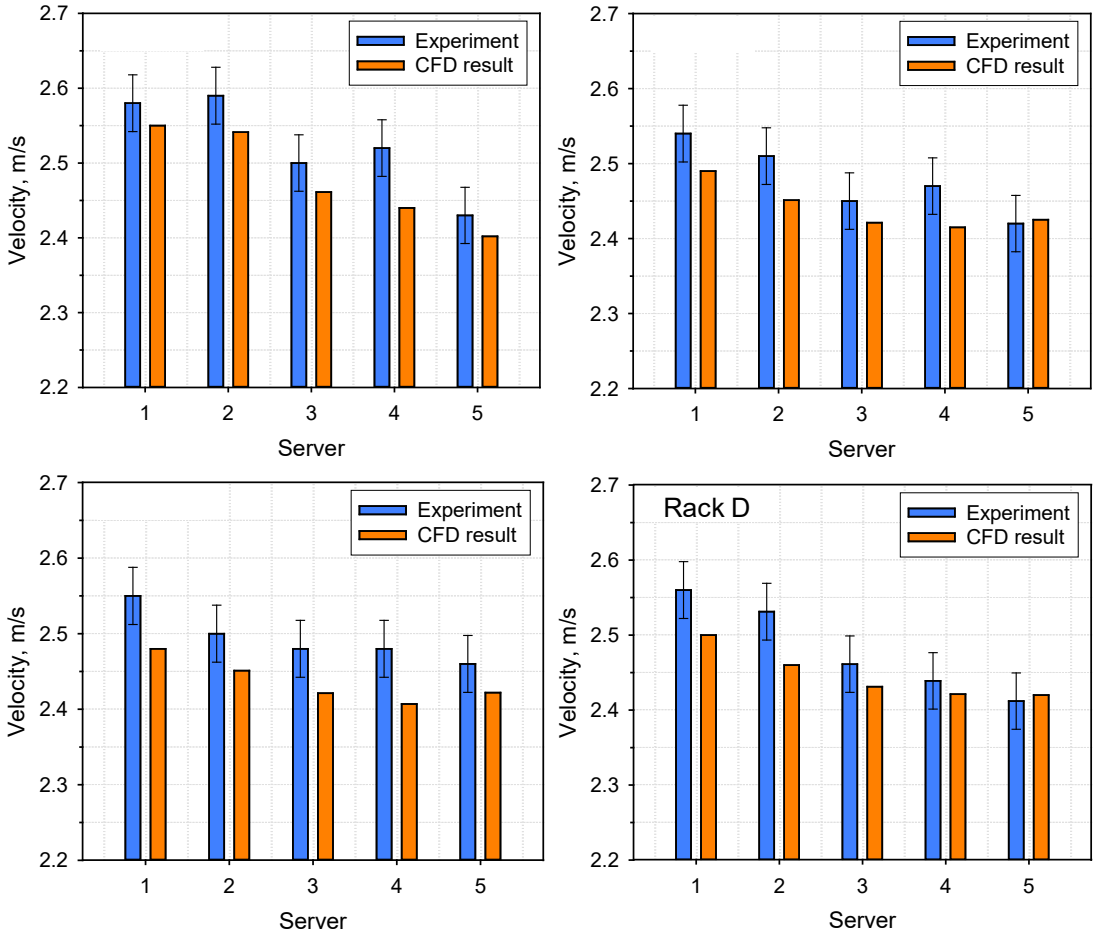

(a)

The short version of the paper (Ref. No. ICAE-61) was presented at ICAE2020, Dec. 1-Dec. 10, Bangkok/Virtual. This paper is a substantial extension of the short version of the conference paper.

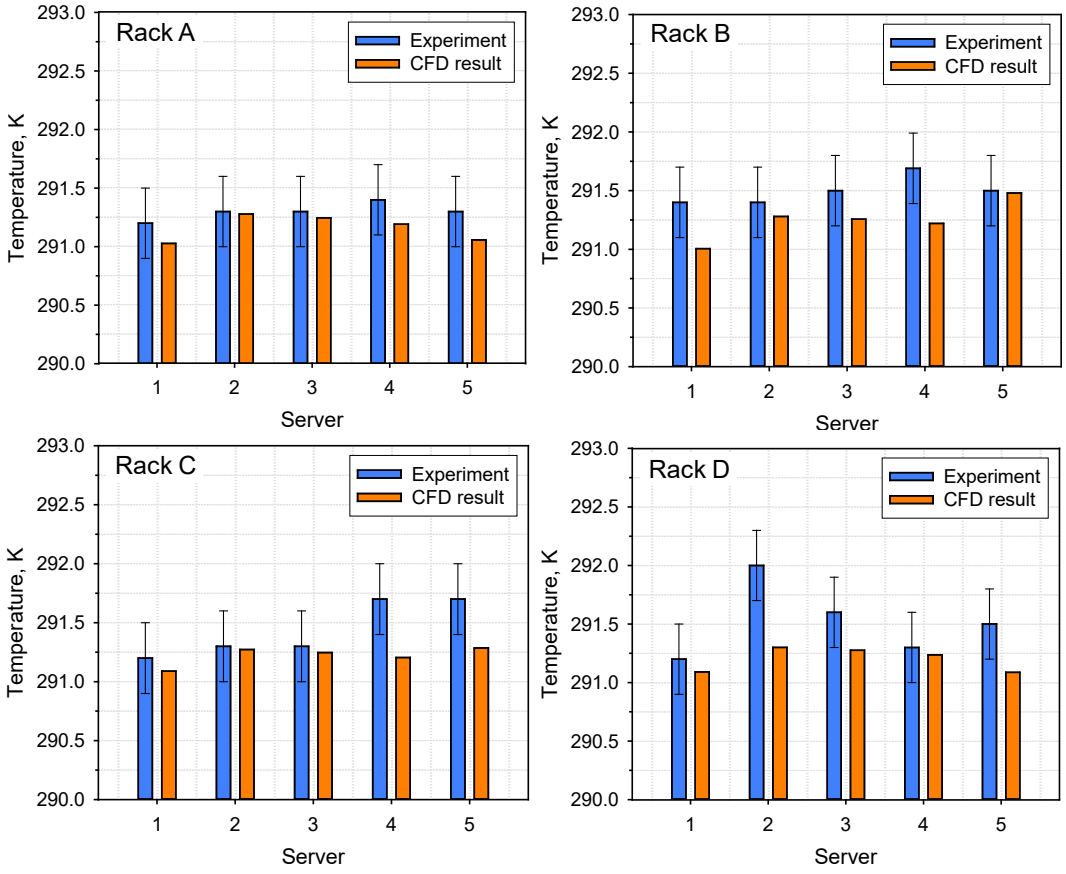

(b)

Figure 6 Comparison between CFD predictions and experimental measurements of averaged inlet (a) air velocities and (b) air temperatures of severs

Table 4 Comparison of simulations and measurements of performance indices

	RCI_{Lo}	RTI	SHI
Experimental data	100%	107.3%	0.08
CFD results	100%	101.6%	0.0

In practice, the power usage effectiveness (PUE) is utilized as an effective indicator to assess the cooling energy consumption of data centers. The PUE can be determined as follows [51].

$$\mathrm{PUE} = \frac{\dot{W}_{AC} + \dot{W}_{IT}}{\dot{W}_{IT}}. \tag{13}$$

Here the PUE value closer to 1 designates all power only used by the IT equipment ($\dot{W}_{IT}$

The short version of the paper (Ref. No. ICAE-61) was presented at ICAE2020, Dec. 1-Dec. 10, Bangkok/Virtual. This paper is a substantial extension of the short version of the conference paper.

$\dot{W}_{AC}$) is computed including the powers associated with the centrifugal fans ($\dot{W}_{cf}$), evaporative water chiller ($\dot{W}_{EWC}$) and water pump ($\dot{W}_{pump}$). The $\dot{W}_{cf}$ equals to $\dot{V}_{cooling}\Delta P_{HX}/\eta$, whereas $\dot{V}_{cooling}$ is the volume flow rate for cooling, ΔP_{HX} is the pressure difference between the air-supply and return ports of HX in the overhead downward flow system, and η is the fan efficiency of 50% referring to the product specifications. The $\dot{W}_{pump}$ values for simulated test data center and proposed large-scale data center are 0.41 kW and 1.11 kW, provided by the manufacturer.

$$\dot{W}_{AC} = \dot{W}_{cf} + \dot{W}_{EWC} + \dot{W}_{pump}. \tag{14}$$

According to the technical data from manufacturer, the selected chiller requires the nominal power involving the compressor ($\dot{W}_{compressor}$) as well as the fan ($\dot{W}_{fan\_spray}$) and pump ($\dot{W}_{pump\_spray}$) of the spray system. The term $\dot{W}_{compressor}$ is calculated by $\dot{Q}_{load}/COP$. Here $\dot{Q}_{load}$ is the heat load of IT equipment, COP is the coefficient of performance of evaporative water chiller. The manufacturer distributes $\dot{W}_{fan\_spray}$ / $\dot{W}_{pump\_spray}$ of 0.68/1.36 kW and 0.23/0.86 kW for the simulated test data center and large-scale data center, respectively.

$$\dot{W}_{EWC} = \dot{W}_{fan\_spray} + \dot{W}_{pump\_spray} + \dot{W}_{compressor}. \tag{15}$$

Besides, the power consumed by the IT equipment ($\dot{W}_{IT}$) includes the powers used by the racks ($\dot{W}_{rack}$) and axial fans ($\dot{W}_{af}$) in the servers. The term $\dot{W}_{rack}$ corresponds to $\dot{Q}_{load}$, while $\dot{W}_{af}$ for the simulated and large-scale data centers are 0.72 kW and 1.44 kW, respectively, from the manufacturing company.

$$\dot{W}_{IT} = \dot{W}_{rack} + \dot{W}_{af}. \tag{16}$$

To determine PUE for the simulated test data center, the additional power uses such as lamps for lighting and fire-fighting system and equipment around the data center are not considered. The measured and predicted PUE results are 1.38 and 1.44, respectively, in this investigation. Overall, the present computational model can properly predict thermofluid characteristics of data centers with reasonable accuracy. Besides, it should be noted that the PUE values range around 1.38-1.55 reported by previous studies using the supportive cooling components integrated with compression refrigeration systems, for instance, Tian, He and Li [26], Han, Sun, Wei, Ji and Xue [28], Ding, He, Hao and Li [52] and Weerts [53]. It can be seen that those systems achieve low PUE results with significant energy savings.

4. Results and discussion

4.1 Air flow distribution

The understanding of inherently complex flow structure is influential to configure the airflow and thermal management of data centers. Figure 7 shows the predicted distributions of (a) velocity

The short version of the paper (Ref. No. ICAE-61) was presented at ICAE2020, Dec. 1-Dec. 10, Bangkok/Virtual. This paper is a substantial extension of the short version of the conference paper.

magnitude, (b) pressure and (c) temperature in the cross section of x= 0.76 m for the simulated test data center. With the same operational scenarios defined in previous section of the grid-independent study, the velocity magnitude contours reveal the vertically downward airflows from the air-supply port of the HX to move along the cold aisle for evenly distributing into each server. In agreement with previous findings of Wang, Tsui and Wang [13] and Chu, Wang, Hsu and Wang [38], the Coanda-like effect tends to produce the recirculating flows appeared over both inlets of upper servers. The airflows are driven utilizing the cooling fans to advance through the servers and blow out at the exit. Under the intensification of buoyant force, the airflows then move upward and restore to the air return port of the HX. Besides, the distributaries redirecting partial airflows to the servers can lead to a successively reduction in the velocity magnitude of downward airflows. In the meantime, the pressure (displayed in Fig. 7(b)) tends to increase gradually from the left to right sides (i.e., 101.4 Pa to 142.3 Pa), producing the roughly same mass flow rate running into each server. The pressure contours also reveal pressure drops across the front and back of ranks having the perforated grilles. In addition, high pressures occurred at the hot aisle become relatively elevated due to the accumulation of hot exhausts under the buoyancy outcomes. Alternatively, the air temperature contours indicate a uniform temperature around 291 K over the cold aisle (in Fig. 7(c)). The airflows then penetrate the servers, resulting in the maximum surface temperatures of copper heat sources up to about 315 K for each server. The heated airflows can infiltrate toward the exits of the racks, deflect upward to merge into hot exhausts, and regress along the hot aisle to the air return port of the overhead downward flow system.

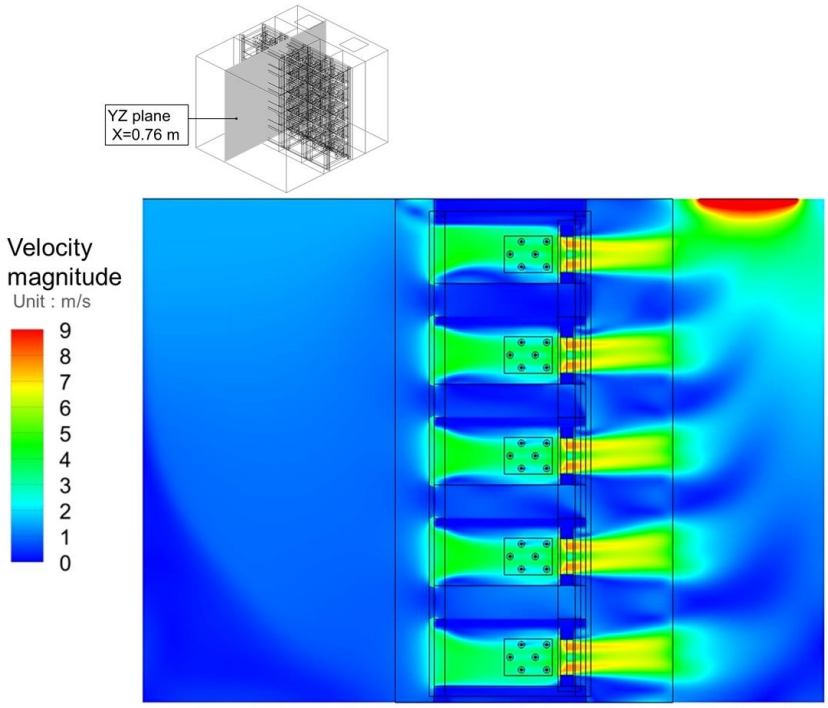

(a)

The short version of the paper (Ref. No. ICAE-61) was presented at ICAE2020, Dec. 1-Dec. 10, Bangkok/Virtual. This paper is a substantial extension of the short version of the conference paper.

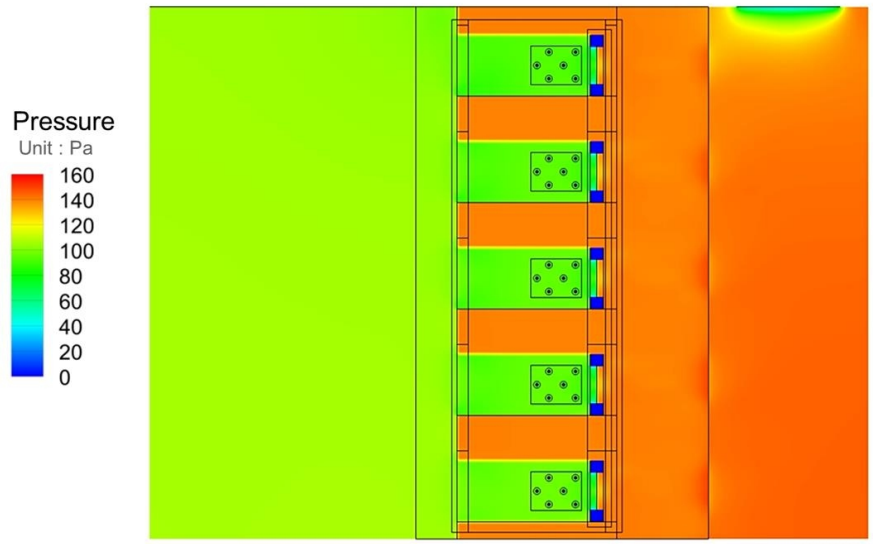

(b)

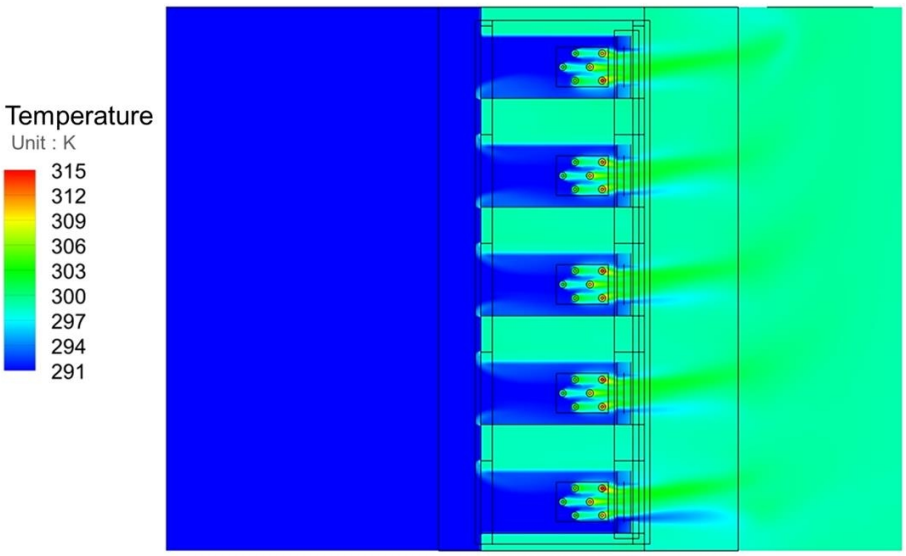

(c)

Figure 7 Predicted distributions of (a) velocity magnitude, (b) pressure and (c) temperature in cross section of x= 0.76 m for simulated test data center

The vertical airflow distribution over each section can substantially influence the heat removal performance of data centers in full-load operations. To evaluate the facility readiness of airflow and thermal management for the large-scale data center to be established in the green energy technology demonstration site, Fig. 8 shows the predicted distributions of (a) velocity magnitude, (b) pressure and (c) temperature in the cross section of x= 3.2 m for the large-scale data center. The CFD results clearly reveal the conditioned air is delivered at high speeds from the air inlet port on the upper area

The short version of the paper (Ref. No. ICAE-61) was presented at ICAE2020, Dec. 1-Dec. 10, Bangkok/Virtual. This paper is a substantial extension of the short version of the conference paper.

of the rack owing to the overhead downward flow layout. The overall airflow pattern is practically symmetric. The airflow distribution ranges 0.75-2.5 m/s from the bottom to the top along the cold aisle, whereas higher airflow speeds of around 2.8-3.5 m/s are observed over the hot aisle (in Fig.8 (a)). Similar to the simulations in the scenario of simulated test data center, those clearly visible recirculating eddies with low velocities appear near the entrance of top servers attributable to the Coanda effect. The elevated exit speeds (up to 9 m/s) of hot aisles tend to entrain heated exhausts issued by the top servers into the air return ports of the racks. The associated velocities of roughly 4.1 m/s at the exits of the top servers are greater than those of other servers. In accordance with the CFD results in the simulated test data center, the predicted pressure contours indicate lower static pressures over the cold aisles of the racks (in Fig. 8(b)), whereas the accumulation of hot exhausts in the hot aisles forms high pressures (102.2-152.0 Pa) for the large-scale data center. Besides, as compared to the scenario of hot aisles on two sides, even higher pressures (of 145-152 Pa) are perceived over the middle hot aisle to expel more heated exhausts via the air return port. In Fig. 8(c), the predictions reveal air of 291 K flowing directly into the cold aisle to develop stable low air temperatures over the whole interior space for fully utilizing the cooling capacity. Alternatively, as described above, the hot aisles are the flow passages having the air exhausted after extracting heat from the servers, and thereby sustain high temperatures of 302-306 K. In addition, the temperature variations across all five servers are fairly consistent in trend, with practically the same exhaust exit temperature.

Effective indicators are vital to assessing the performance of flow and thermal managements for devising data centers. The thermal performance indices of RCI_{Lo} (the subscript Lo represents the temperature conditions at low end of temperature range [54]), SHI, RTI are required to evaluate the thermal performance of the large-scale data center [55]. In effect, the ideal values of RCI_{Lo}, SHI and RTI are 100%, close to zero and 1, respectively, suggesting no indication of improper mixing of hot and cold airflows within the racks. The predictions assess RCI_{Lo} of 100%, SHI of 0 and RTI of 102% for the large-scale data center, complying with the ideal environmental conditions recommended by ASHRAE TC 99 [40], The estimate of RTI= 102% shows the presence of insignificant return hot airflows in the racks. Nevertheless, the arrangements of detaching the hot and cold aisles as well as eliminating the raised floor can circumvent the mixing and short passage of airflows. Hence, the overhead downward flow system has confirmed its effectiveness of using the cold aisle containment (CAC) design to make high performance metrics in thermal management and airflow distribution.

The short version of the paper (Ref. No. ICAE-61) was presented at ICAE2020, Dec. 1-Dec. 10, Bangkok/Virtual. This paper is a substantial extension of the short version of the conference paper.

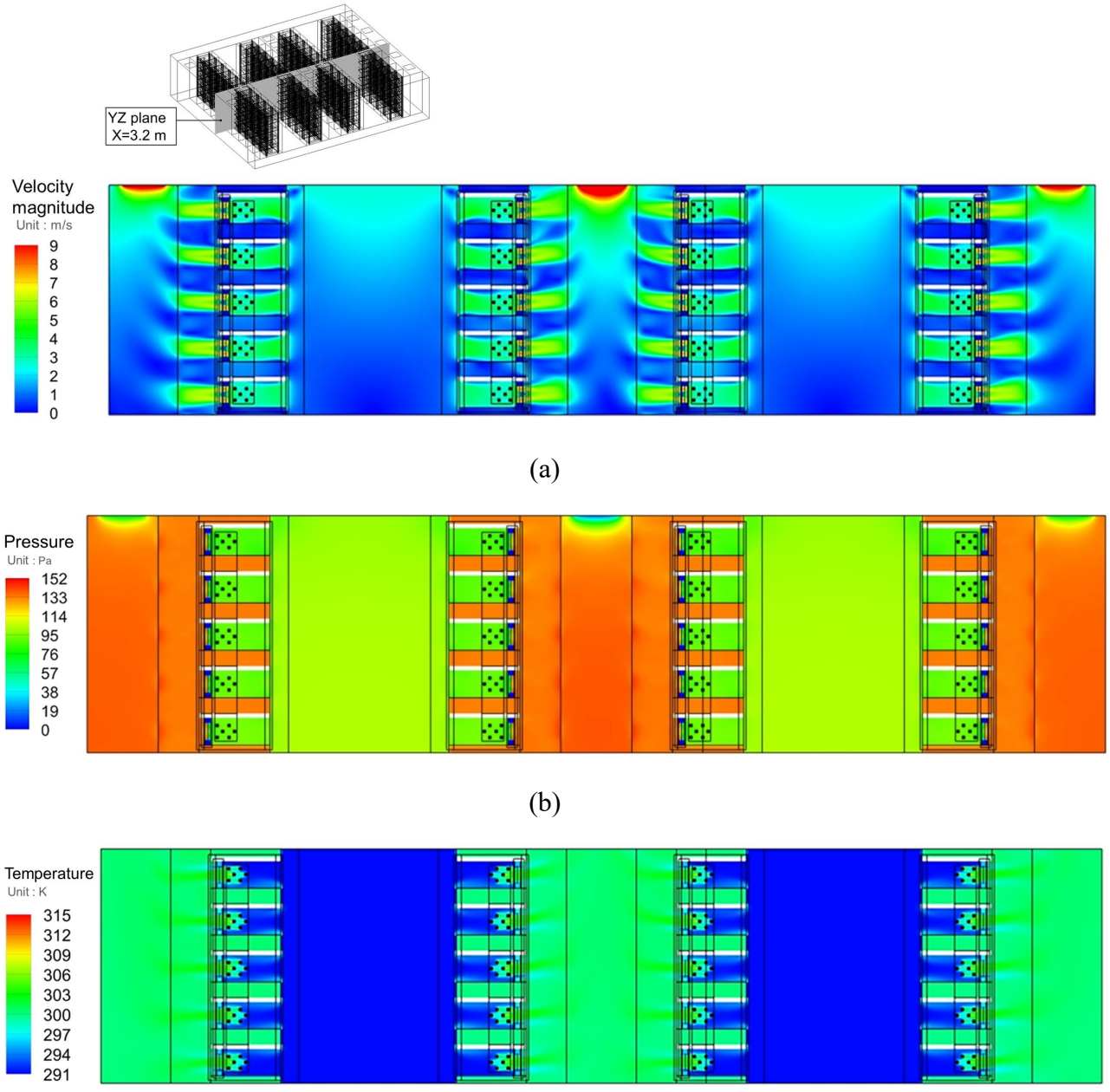

Figure 8 Predicted distributions of (a) velocity magnitude, (b) pressure and (c) temperature in cross section of x= 3.2 m for large-scale data center

4.2 Effect of inlet air temperature

The temperature of supply air can affect the thermal performance of data centers in operations. Practically, the inlet air temperature plays an important role in the cooling of the large-scale data center. According to the recommendation by ASHRAE TC 99 [40], the temperature of supply air should be well maintained within 18-27 °C (291-300 K) to achieve satisfactory cooling outcomes

The short version of the paper (Ref. No. ICAE-61) was presented at ICAE2020, Dec. 1-Dec. 10, Bangkok/Virtual. This paper is a substantial extension of the short version of the conference paper.

of thermal control for data centers. Figure 9 demonstrates the predicted temperature distributions in the cross section of x= 3.2 m at the inlet air temperatures of (a) 291 K, (b) 295 K and (c) 300 K for the large-scale data center. In essence, the outlet temperatures of air return ports in the hot aisles tend to increase linearly with the inlet temperatures due to the identical delivery air velocity of 2.54 m/s. For three different inlet air temperature settings, it is noticed that the nearly same temperature differences of the inlet and outlet air temperatures of the racks to transfer the heating power of all severs, producing comparable thermal effectiveness of data centers. This study further explores the performance indices for the outcomes of air distribution and heat transfer management. Table 5 illustrates the estimated performance indices at different inlet air temperatures for the large-scale data center. In effect, the variations of supply air temperatures reveal insignificant impacts on the temperature uniformity over the cold and hot aisles in conjunction with the associated thermal performance.

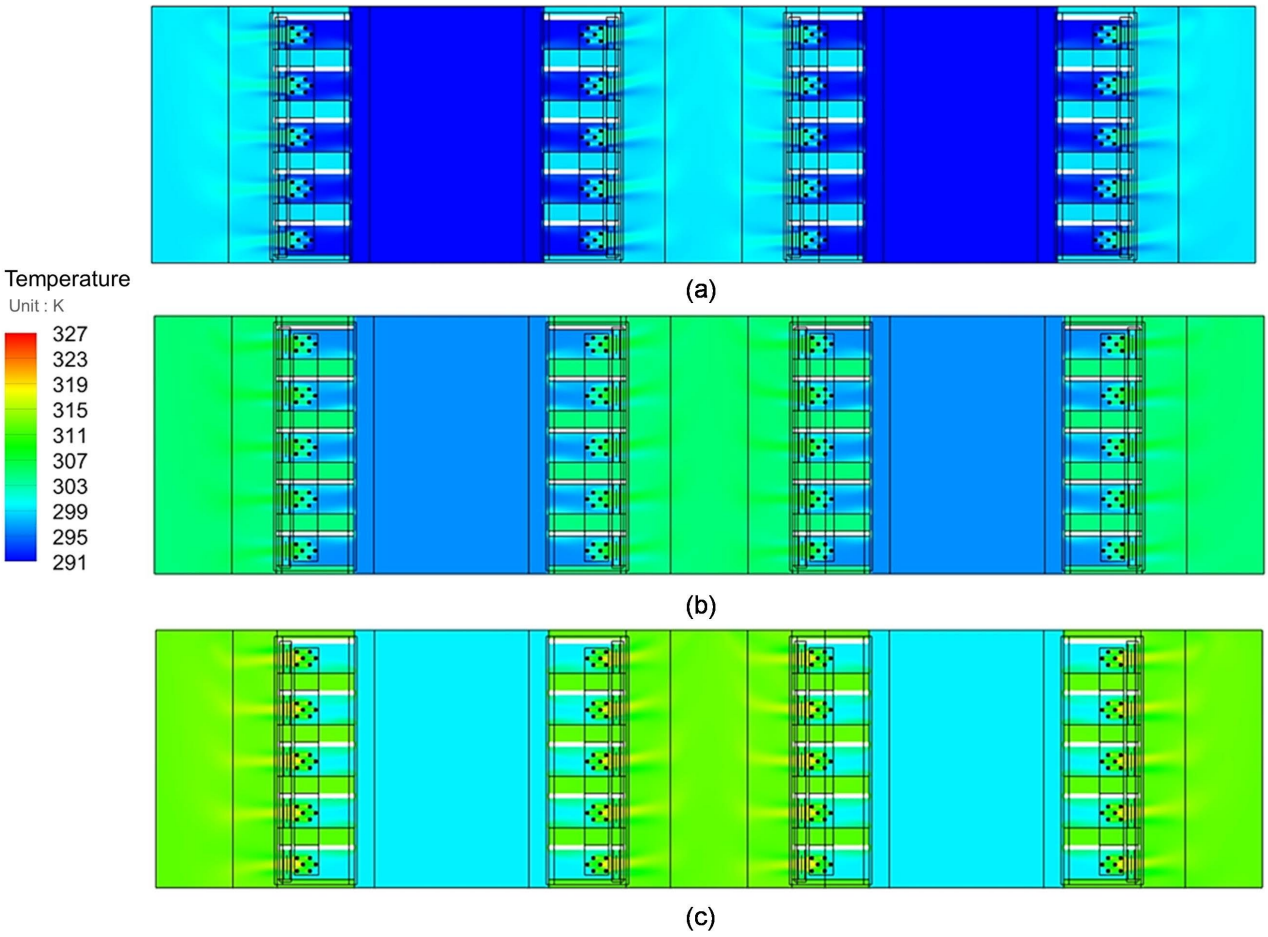

Figure 9 Predicted temperature distributions in cross section of x= 3.2 m at inlet air temperatures of (a) 291 K, (b) 295 K and (c) 300 K for large-scale data center

The short version of the paper (Ref. No. ICAE-61) was presented at ICAE2020, Dec. 1-Dec. 10, Bangkok/Virtual. This paper is a substantial extension of the short version of the conference paper.

Table 5 Estimated performance indices at different inlet air temperatures for large-scale data center

Inlet air temperature	RCI_{Lo}	SHI	RTI
291 K	100%	0.0	102.8%
295 K	100%	0.0	103.1%
300 K	100%	0.0	103.3%

4.3 Effect of inlet air velocity

The inlet air velocity is the critical operating parameter closely related to the regulation of air distribution inside the racks. In practice, the proper temperature difference between the supply and return air temperatures of the heat exchanger should be well within 11°C to achieve reasonable thermal performance, as suggested by Samadiani, Joshi, Allen and Mistree [56]. Having the fixed total heat power for all racks with the given areas of air-supply ports, this study arranges the temperature difference of 5-11°C, and thereby determine the corresponding inlet air velocities ranging from 1.85 m/s to 4.06 m/s. Figure 10 presents the predicted temperature distributions in the cross section of x= 3.2 m at the inlet air velocity for (a) 1.85 m/s, (b) 2.54 m/s and (c) 4.06 m/s for the large-scale data center. For the inlet velocity of 1.85 m/s (in Fig. 10(a)), the temperature contours reveal a fairly uniform low temperature of 18°C (291 K) for the cold aisles of the racks. The combined effects of returning airflows (with high temperatures of 298.7-299.1 K) from the hot aisles into the cold aisles via the 0.5-cm gaps as well as the deficient inertial momentum resulting from relatively low inlet velocities of supply air can induce local recirculation of heated airflows appeared over the upstream regions inside the servers. In addition, the elevated temperatures (around 307 K) over the hot aisles lead to the resultant temperature differences of hot and cold aisles up to 16 K. Accordingly, the settings at low inlet air velocities can operate the IT equipment under inappropriate environmental conditions, deteriorating the thermal performance of the large-scale data center. As compared to the scenario of 1.85 m/s, increased inlet air velocities to 2.54 m/s and 4.06 m/s notably reduce the temperatures by 5-9 K over the hot aisles (in Fig. 10(b) and (c)). This can be attributed to the heat transfer balance between the total heating power of severs and the heat airflow rates from the inlets to the outlets of racks. The CFD predictions show the outcomes of improved overall temperature uniformity by raising the supply air velocity. Moreover, the escalation of delivered air flowrates tends to augment the pressure in the cold aisles, and thereby drive the cold airflows running through the servers to the hot aisles with the disappearance of recirculating flows described above.

Table 6 shows the estimated performance indices at different inlet air velocities for the large-scale data center. First of all, the operating settings of inlet air temperature well comply with the recommended range of the ASHRAE TC 99 [40], maintaining RCI_{Lo} of 100% under varied inlet air

The short version of the paper (Ref. No. ICAE-61) was presented at ICAE2020, Dec. 1-Dec. 10, Bangkok/Virtual. This paper is a substantial extension of the short version of the conference paper.

velocities. However, the associated SHI/RTI values increase from 0.0/102.8% to 0.18/132.5% with respect to the decline of supplied air velocity from 2.54 m/s to 1.85 m/s. In effect, low delivery air flow rates can induce hot reversal airflows, and thereby cause the improper temperature distribution, depreciating the outcomes of air distribution and thermal management in terms of the unfavorable SHI and RTI values. On the other hand, the scenario with a high speed of 4.06 m/s tends to develop relatively higher pressures at cold aisles to push the cold airflows further downstream in the severs, producing the reduced outlet temperatures of return air ports with a lower RTI value of 98.6%.

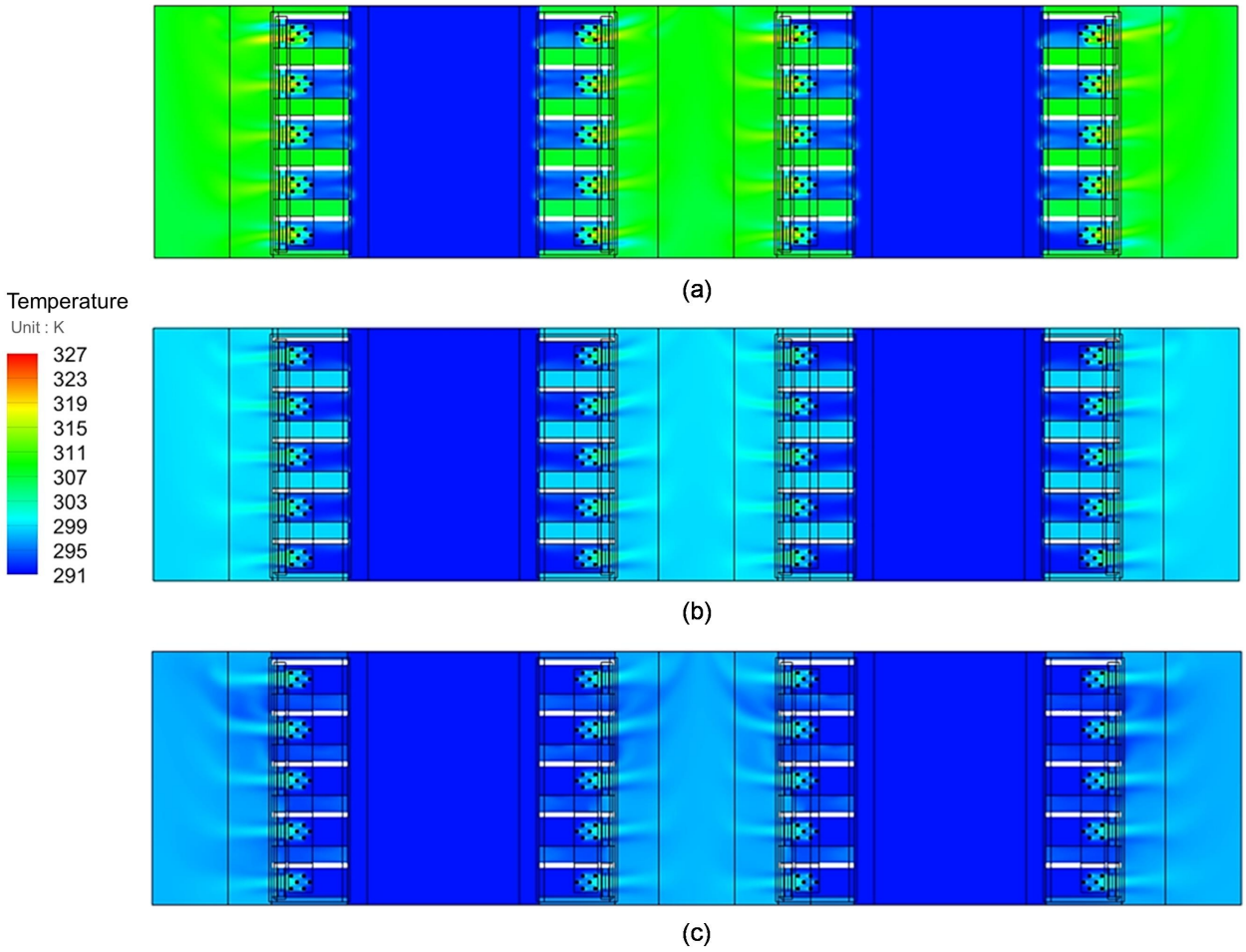

Figure 10 Predicted temperature distributions in cross section of x= 3.2 m at inlet air velocities of (a) 1.85 m/s, (b) 2.54 m/s and (c) 4.06 m/s for large-scale data center

The short version of the paper (Ref. No. ICAE-61) was presented at ICAE2020, Dec. 1-Dec. 10, Bangkok/Virtual. This paper is a substantial extension of the short version of the conference paper.

Table 6 Estimated performance indices at different inlet air velocities for large-scale data center

Inlet air velocity	RCI_{Lo}	SHI	RTI
1.85 m/s	100%	0.18	132.5%
2.54 m/s	100%	0.0	102.8%
4.06 m/s	100%	0.0	98.6%

4.4 Effect of climatic conditions

The meteorological parameters can appreciably affect the operating performance of data center attributable to its cooling energy use closely related to the geographic location indicated by Bulut and Aktacir [57], Cho, Lim and Kim [58] and Lee and Chen [59]. Table 7 summarizes the power ratings consumed by air-conditioning components of the large-scale data center, provided by the manufacturers. In addition, the cooling system performance of the data center can be varied under different environmental properties. Table 8 presents the monthly average dry-bulb temperature and relative humidity from the Shalun meteorological station, Tainan, Taiwan. The climatic conditions are extracted from the database measured from 2015 to 2020.

Table 7 Air-conditioning power consumption of large-scale data center

Component	Parameter	Value per set
Room	Number of racks	40
	Heat transfer rate per rack	9 kW
	Axial fans power per server	0.052 kW
Evaporative water chiller system (4 sets) (JEW-30F/Jesan, Pulse-Luxe, Taiwan)	Heat flow dissipation capacity per set	90 kW
	Fan nominal power consumption per set	1.36 kW
	Pump power consumption per set	0.86 kW
Water pump (5 sets) (YT×2", Yongda Pumping, Taiwan)	Power consumption per set	1.11 kW
	Maximum water flow rate per set	104 LPM
Centrifugal fan (20 sets) (ZIEHL-ABEGG, Germany)	Fan nominal power consumption per set	1.81 kW

The short version of the paper (Ref. No. ICAE-61) was presented at ICAE2020, Dec. 1-Dec. 10, Bangkok/Virtual. This paper is a substantial extension of the short version of the conference paper.

Table 8 Monthly average dry-bulb temperature and relative humidity at Shalun meteorological station

January		February		March		April		May		June	
T,℃	RH	T,℃	RH	T,℃	RH	T,℃	RH	T,℃	RH	T,℃	RH
18.8	0.81	19.9	0.78	23.3	0.76	23.5	0.74	28.2	0.79	30	0.73
July		August		September		October		November		December	
T,℃	RH	T,℃	RH	T,℃	RH	T,℃	RH	T,℃	RH	T,℃	RH
29.9	0.76	28.3	0.84	28.8	0.75	26.8	0.75	22.2	0.81	20.3	0.80

Referring to the technical data from the manufactures, Fig. 11 illustrates the effect of climate conditions on the profiles of the required average monthly energy use for different air-conditioning components for the large-scale data center. In effect, we observe a noticeable decrease in the power use of evaporative water chiller as the coefficient of performance (COP) increases during the winter season, suggesting to be the component mainly affected by the state of the atmosphere. On the other hand, the centrifugal fans and water pumps reveal constant power use profiles regardless of climate conditions due to their stable thermal performance without influenced by the environmental impact. Therefore, the overall power use levels can be primarily dependent on the chiller load. Table 9 illustrtes the monthly COP variations of the evaporative water chiller of the air-conditioning system, indicating the annual power required to dissipate the heat from the severs. In the period of months from June to September, it is noted that the less cooling capacities with low COP values of around 3.62 during this hot season. Then, a relatively increase in COP values ranging 3.84–4.05 occurs during the transition months of April, May, and October. The COP values of 4.13–4.23 can realize a reduction in cooling power for energy saving during the period of cold season (especially December to Feberary).

The short version of the paper (Ref. No. ICAE-61) was presented at ICAE2020, Dec. 1-Dec. 10, Bangkok/Virtual. This paper is a substantial extension of the short version of the conference paper.

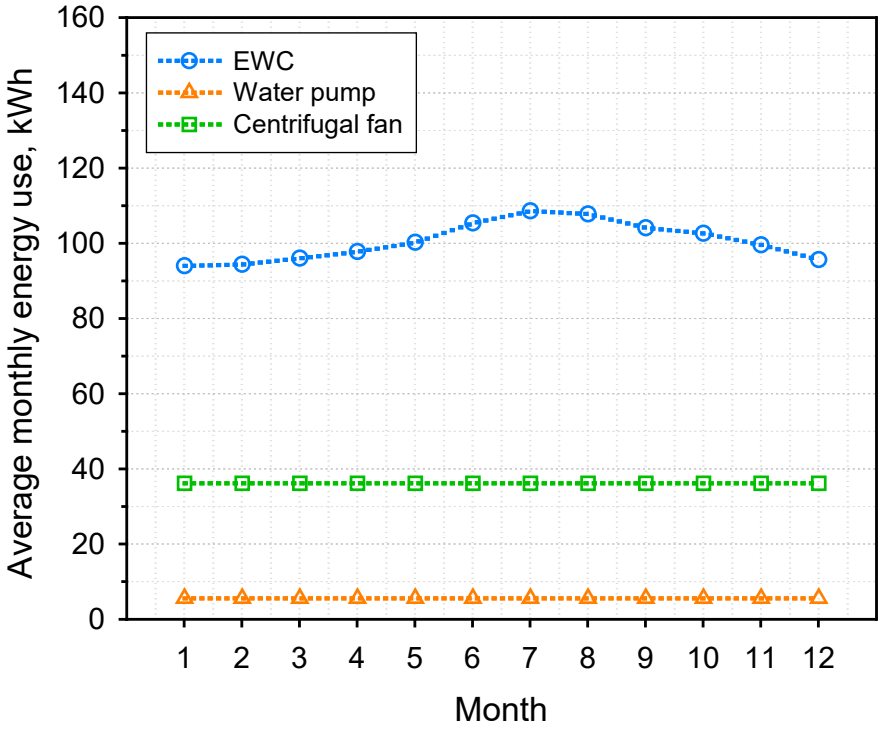

Figure 11 Effect of climate conditions on profiles of required average monthly energy use for different air-conditioning components for large-scale data center

Table 9 Monthly COP variations of evaporative water chiller

Month	Jan.	Feb.	Mar.	Apr.	May.	Jun.
COP	4.23	4.21	4.13	4.05	3.94	3.73
Month	Jul.	Aug.	Sep.	Oct.	Nov.	Dec.
COP	3.62	3.64	3.78	3.84	3.97	4.15

The air-conditioning power consumption of the planned large-scale data center can be affected by the outside climate conditions. Figure 12 displays the effect of climate conditions on the annual PUE profile. In general, the PUE values range from 1.35 to 1.41 throughout the year for the large-scale data center to be constructed in the green energy technology demonstration site of the Shalun smart green energy science city. Based on the earlier results presented by Chu, Wang, Hsu and Wang [38] and Herrlin [39], the worldwide average PUE statistics from 2000 to 2010 range 1.83-1.92 for general cooling systems of data centers. The maximum PUE value reaches 1.41 in

The short version of the paper (Ref. No. ICAE-61) was presented at ICAE2020, Dec. 1-Dec. 10, Bangkok/Virtual. This paper is a substantial extension of the short version of the conference paper.

July because of high cooling energy use during the summer period. The results show that the estimated PUE of large-scale data center in the hot season is still lower than the above worldwide average PUE data, revealing the better thermal performance as expected for the proposed data center design in cooling operations. In contrast, PUE is greatly decreased with the lowest value of 1.35 in winter, indicating a peak discrepancy of 4.20% compared with the power usage in summer. Overall, the calculated average PUE of 1.38 for the large-scale data center is substantially less than the average PUE value of 1.59 reported by "Uptime institute global data center survey 2020" [51], demonstrating the potential savings of cooling energy and cost.

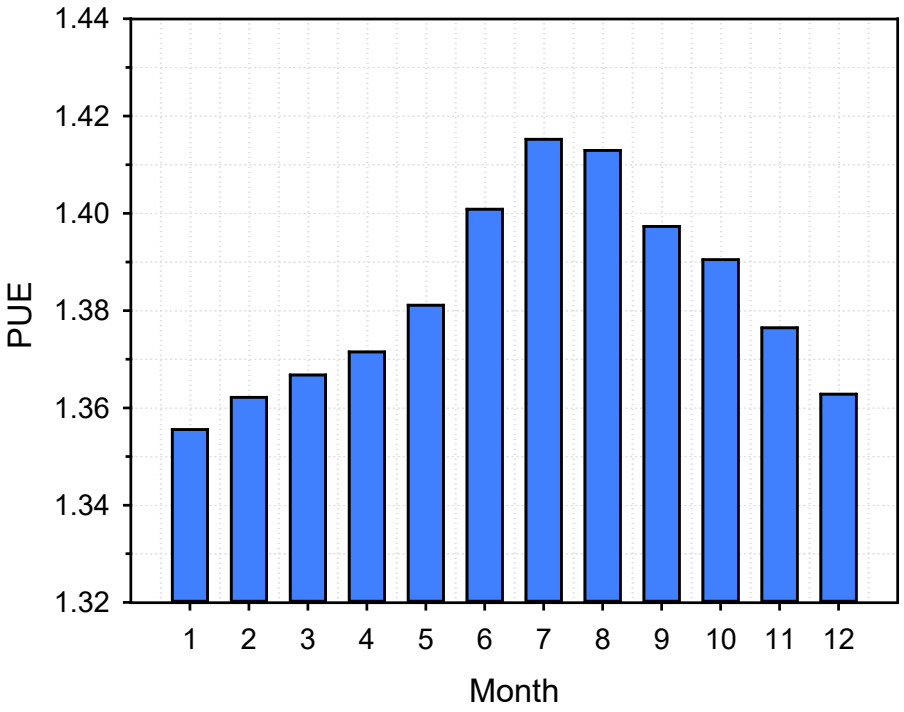

Figure 12 Effect of climate conditions on annual PUE profile for large-scale data center

5. Conclusions

This study presents a container data center via the cold aisle containment design combining with a HX on the airside and a EWC on the waterside as an effective solution to enhance the operational performance of existing and future data centers used in tropical and subtropical areas. CFD simulations are conducted to assess the temperature distributions and thermal performance at varying inlet air temperatures and velocities for the proposed large-scale data center. The power usage effectiveness (PUE) is also examined under variable climatic conditions. The conclusions are summarized below.

(1)The simulations are consistent with the measured averaged inlet air velocities, temperatures and

The short version of the paper (Ref. No. ICAE-61) was presented at ICAE2020, Dec. 1-Dec. 10, Bangkok/Virtual. This paper is a substantial extension of the short version of the conference paper.

performance indices, revealing the reasonably accurate predictions of thermofluid characteristics of the simulated test data centers.

(2)The operation of the large-scale data center using the overhead downward flow system with cold aisle containment achieves RCI_{Lo} of 100%, SHI of 0 and RTI of 102%, indicating a significant improvement of air distribution and thermal management.

(3)The temperature uniformity over the cold and hot aisles can result in the minor impacts of supply air temperature variations on the thermal performance indices for the large-scale data center.

(4)The inlet air velocity has dominant effect on the air distribution and thermal management of data centers. A high supply air velocity (of 4.06 m/s) can effectively improve the overall temperature uniformity and eliminate the recirculating flow phenomenon with a lower RTI value of 98.6%.

(5)In view of the monthly COP variations of EWC for the air-conditioning system, the highest PUE value of 1.41 occurs in July during summer, while PUE has the lowest value of 1.35 in winter. The estimated average PUE of 1.38 is evidently lower than the average PUE of 1.59 referring to the results of 2020 data center industry survey for the potential reduction of energy consumption.

Acknowledgment

This study represents part of the results obtained under the support of Ministry of Science and Technology, Taiwan, ROC (Contract No. MOST109-3116-F-027-001-CC1).

References

[1] Mitchell-Jackson J, Koomey JG, Nordman B, Blazek M. Data center power requirements: measurements from Silicon Valley. Energy. 2003;28:837-50.

[2] Cho J, Woo J. Development and experimental study of an independent row-based cooling system for improving thermal performance of a data center. Applied Thermal Engineering. 2020;169:114857.

[3] Shehabi A, Smith S, Sartor D, Brown R, Herrlin M, Koomey J, et al. United states data center energy usage report. 2016.

[4] Lima JM. Data centres of the world will consume 1/5 of earth's power by 2025. Data Economy. 2017.

[5] Rong H, Zhang H, Xiao S, Li C, Hu C. Optimizing energy consumption for data centers. Renewable and Sustainable Energy Reviews. 2016;58:674-91.

[6] Greenberg S, Mills E, Tschudi B, Rumsey P, Myatt B. Best practices for data centers: Lessons learned from benchmarking 22 data centers. Proceedings of the ACEEE Summer Study on Energy Efficiency in Buildings in Asilomar, CA ACEEE, August. 2006;3:76-87.

[7] Belady C, Rawson A, Pfleuger J, Cader T. Green grid data center power efficiency metrics: PUE and DCIE. Technical report, Green Grid; 2008.

The short version of the paper (Ref. No. ICAE-61) was presented at ICAE2020, Dec. 1-Dec. 10, Bangkok/Virtual. This paper is a substantial extension of the short version of the conference paper.

[8] Cho J, Kim Y. Improving energy efficiency of dedicated cooling system and its contribution towards meeting an energy-optimized data center. Applied energy. 2016;165:967-82.
[9] Park J, Director DCD. Data Center v1. 0. Open Compute Project. 2011.
[10] Díaz AJ, Cáceres R, Torres R, Cardemil JM, Silva-Llanca L. Effect of climate conditions on the thermodynamic performance of a data center cooling system under water-side economization. Energy and Buildings. 2020;208:109634.
[11] Cho J, Yang J, Lee C, Lee J. Development of an energy evaluation and design tool for dedicated cooling systems of data centers: Sensing data center cooling energy efficiency. Energy and Buildings. 2015;96:357-72.
[12] Lu H, Zhang Z, Yang L. A review on airflow distribution and management in data center. Energy and Buildings. 2018;179:264-77.
[13] Wang C-H, Tsui Y-Y, Wang C-C. On cold-aisle containment of a container datacenter. Applied Thermal Engineering. 2017;112:133-42.
[14] Nada S, Elfeky K. Experimental investigations of thermal managements solutions in data centers buildings for different arrangements of cold aisles containments. Journal of building engineering. 2016;5:41-9.
[15] Gondipalli S, Bhopte S, Sammakia B, Iyengar MK, Schmidt R. Effect of isolating cold aisles on rack inlet temperature. 2008 11th Intersociety Conference on Thermal and Thermomechanical Phenomena in Electronic Systems: IEEE; 2008. p. 1247-54.
[16] Lu T, Lü X, Remes M, Viljanen M. Investigation of air management and energy performance in a data center in Finland: Case study. Energy and Buildings. 2011;43:3360-72.
[17] Khalaj AH, Scherer T, Siriwardana J, Halgamuge S. Increasing the thermal efficiency of an operational data center using cold aisle containment. 7th International Conference on Information and Automation for Sustainability: IEEE; 2014. p. 1-6.
[18] Gao C, Yu Z, Wu J. Investigation of airflow pattern of a typical data center by CFD simulation. Energy Procedia. 2015;78:2687-93.
[19] Schmidt RR, Iyengar M, Vogel M, Pienta B. Comparison between underfloor supply and overhead supply ventilation designs for data center high-density clusters/discussion. ASHRAE Transactions. 2007;113:115.
[20] Han Z, Zhang Y, Meng X, Liu Q, Li W, Han Y, et al. Simulation study on the operating characteristics of the heat pipe for combined evaporative cooling of computer room air-conditioning system. Energy. 2016;98:15-25.

The short version of the paper (Ref. No. ICAE-61) was presented at ICAE2020, Dec. 1-Dec. 10, Bangkok/Virtual. This paper is a substantial extension of the short version of the conference paper.

[21] Harby K, Gebaly DR, Koura NS, Hassan MS. Performance improvement of vapor compression cooling systems using evaporative condenser: An overview. Renewable and sustainable energy reviews. 2016;58:347-60.
[22] Han Z, Ji Q, Wei H, Xue D, Sun X, Zhang X, et al. Simulation study on performance of data center air-conditioning system with novel evaporative condenser. Energy. 2020;210:118521.
[23] Masanet E, Shehabi A, Lei N, Smith S, Koomey J. Recalibrating global data center energy-use estimates. Science. 2020;367:984-6.
[24] Okazaki T, Seshimo Y. Cooling system using natural circulation for air conditioning. Transactions of the Japan Society of Refrigerating and Air Conditioning Engineers. 2011;25:239-51.
[25] Sun X, Zhang Q, Medina MA, Liao S. Performance of a free-air cooling system for telecommunications base stations using phase change materials (PCMs): in-situ tests. Applied Energy. 2015;147:325-34.
[26] Tian H, He Z, Li Z. A combined cooling solution for high heat density data centers using multi-stage heat pipe loops. Energy and Buildings. 2015;94:177-88.
[27] Lu Q, Jia L. Experimental study on rack cooling system based on a pulsating heat pipe. Journal of Thermal Science. 2016;25:60-7.
[28] Han Z, Sun X, Wei H, Ji Q, Xue D. Energy saving analysis of evaporative cooling composite air conditioning system for data centers. Applied Thermal Engineering. 2021;186:116506.
[29] Jahangir MH, Mokhtari R, Mousavi SA. Performance evaluation and financial analysis of applying hybrid renewable systems in cooling unit of data centers–A case study. Sustainable Energy Technologies and Assessments. 2021;46:101220.
[30] Zhang H, Shao S, Xu H, Zou H, Tian C. Integrated system of mechanical refrigeration and thermosyphon for free cooling of data centers. Applied Thermal Engineering. 2015;75:185-92.
[31] Oro E, Codina M, Salom J. Energy model optimization for thermal energy storage system integration in data centres. Journal of Energy Storage. 2016;8:129-41.
[32] Ling L, Zhang Q, Yu Y, Ma X, Liao S. Energy saving analysis of the cooling plant using lake water source base on the optimized control strategy with set points change. Applied Thermal Engineering. 2018;130:1440-9.
[33] Liu Y, Yang X, Li J, Zhao X. Energy savings of hybrid dew-point evaporative cooler and micro-channel separated heat pipe cooling systems for computer data centers. Energy. 2018;163:629-40.

The short version of the paper (Ref. No. ICAE-61) was presented at ICAE2020, Dec. 1-Dec. 10, Bangkok/Virtual. This paper is a substantial extension of the short version of the conference paper.

[34] Zhou F, Li C, Zhu W, Zhou J, Ma G, Liu Z. Energy-saving analysis of a case data center with a pump-driven loop heat pipe system in different climate regions in China. Energy and Buildings. 2018;169:295-304.
[35] Hwang Y, Radermacher R, Kopko W. An experimental evaluation of a residential-sized evaporatively cooled condenser. International journal of refrigeration. 2001;24:238-49.
[36] Lee Y-T, Hong S, Chien L-H, Lin W-H, Yang A-S. Liquid film dispersion on horizontal circular tubes under spray impingement. International Journal of Heat and Mass Transfer. 2020;160:120223.
[37] Standard A. Standard 41.2-1987, Standard methods for laboratory air-flow measurement. American Society of Heating, Refrigerating and Air-Conditioning Engineers, Inc, Atlanta. 1987.
[38] Chu W-X, Wang R, Hsu P-H, Wang C-C. Assessment on rack intake flowrate uniformity of data center with cold aisle containment configuration. Journal of Building Engineering. 2020;30:101331.
[39] Herrlin MK. Rack cooling effectiveness in data centers and telecom central offices: The rack cooling index (RCI). Transactions-American Society of Heating Refrigerating and Air conditioning Engineers. 2005;111:725.
[40] TC A. Data center power equipment thermal guidelines and Best practices. ASHRAE TC 99, ASHRAE, USA. 2016.
[41] Herrlin MK. Improved data center energy efficiency and thermal performance by advanced airflow analysis. Digital power forum2007. p. 10-2.
[42] Sharma R, Bash C, Patel C. Dimensionless parameters for evaluation of thermal design and performance of large-scale data centers. 8th AIAA/ASME Joint thermophysics and heat transfer conference2002. p. 3091.
[43] Shih T-H, Liou WW, Shabbir A, Yang Z, Zhu J. A new k-epsilon eddy viscosity model for high Reynolds number turbulent flows: Model development and validation. NASA Sti/recon Technical Report N. 1994;95:11442.
[44] Jang D, Jetli R, Acharya S. Comparison of the PISO, SIMPLER, and SIMPLEC algorithms for the treatment of the pressure-velocity coupling in steady flow problems. Numerical Heat Transfer, Part A: Applications. 1986;10:209-28.
[45] Lin C-C, Shih Y-C. The optimal thermal management study of a next-generation data center. Case Studies in Thermal Engineering. 2021;26:101031.
[46] Lu H, Zhang Z. Numerical and experimental investigations on the thermal performance of a data center. Applied Thermal Engineering. 2020;180:115759.

The short version of the paper (Ref. No. ICAE-61) was presented at ICAE2020, Dec. 1-Dec. 10, Bangkok/Virtual. This paper is a substantial extension of the short version of the conference paper.

[47] Gupta R, Asgari S, Moazamigoodarzi H, Pal S, Puri IK. Cooling architecture selection for air-cooled Data Centers by minimizing exergy destruction. Energy. 2020;201:117625.
[48] Jin C, Bai X. The study of servers' arrangement and air distribution strategy under partial load in data centers. Sustainable Cities and Society. 2019;49:101617.
[49] Tradat MI, Sammakia BG, Hoang CH, Alissa HA. An experimental and numerical investigation of novel solution for energy management enhancement in data centers using underfloor plenum porous obstructions. Applied Energy. 2021;289:116663.
[50] Chu W-X, Hsu C-S, Tsui Y-Y, Wang C-C. Experimental investigation on thermal management for small container data center. Journal of Building Engineering. 2019;21:317-27.
[51] Ascierto R, Lawrence A. Uptime institute global data center survey 2020. Uptime Institute. 2020;2.
[52] Ding T, He Z, Hao T, Li Z. Application of separated heat pipe system in data center cooling. Applied Thermal Engineering. 2016;109:207-16.
[53] Weerts BA. NSIDC green data center project: Coolerado and modeling an application of the Maisotsenko cycle: University of Colorado at Boulder; 2012.
[54] Gong X, Zhang Z, Gan S, Niu B, Yang L, Xu H, et al. A review on evaluation metrics of thermal performance in data centers. Building and Environment. 2020;177:106907.
[55] Zhang K, Zhang Y, Liu J, Niu X. Recent advancements on thermal management and evaluation for data centers. Applied thermal engineering. 2018;142:215-31.
[56] Samadiani E, Joshi Y, Allen JK, Mistree F. Adaptable robust design of multi-scale convective systems applied to energy efficient data centers. Numerical Heat Transfer, Part A: Applications. 2010;57:69-100.
[57] Bulut H, Aktacir MA. Determination of free cooling potential: A case study for Istanbul, Turkey. Applied Energy. 2011;88:680-9.
[58] Cho J, Lim T, Kim BS. Viability of datacenter cooling systems for energy efficiency in temperate or subtropical regions: Case study. Energy and buildings. 2012;55:189-97.
[59] Lee K-P, Chen H-L. Analysis of energy saving potential of air-side free cooling for data centers in worldwide climate zones. Energy and buildings. 2013;64:103-12.

The short version of the paper (Ref. No. ICAE-61) was presented at ICAE2020, Dec. 1-Dec. 10, Bangkok/Virtual. This paper is a substantial extension of the short version of the conference paper.

Nomenclature

ASHRAE	American Society of Heating, Refrigerating and Air-conditioning Engineers
C	Specific heat
CAC	Cold aisle containment
COP	Coefficient of performance
CRAC	Computer room air-conditioner
EWC	Evaporative water chiller
$\vec{g}$	Gravitational acceleration
HX	Heat exchanger
k	Turbulent kinetic energy dissipation rate
n	Number of rack
PUE	Power usage efficiency
p	Pressure
ΔP	Pressure drop
Q	Volume flow rate
RCI	Rack cooling index
RTI	Return temperature index
T	Temperature
T_R	Outlet temperatures from the HXs
T_s	Inlet temperatures from the HXs
T_x	Mean intake temperature into the racks
ΔT_{Equip}	Weighted average temperature rise across the equipment
SHI	Supply heat index
$\vec{V}$	Velocity vector
V	Velocity magnitude
W	Power consumption

The short version of the paper (Ref. No. ICAE-61) was presented at ICAE2020, Dec. 1-Dec. 10, Bangkok/Virtual. This paper is a substantial extension of the short version of the conference paper.

β	Thermal expansion coefficient
ε	Turbulent energy dissipation rate
ρ	Density
λ_{eff}	Effective thermal conductivity
μ_{eff}	Effective dynamic viscosity

The short version of the paper (Ref. No. ICAE-61) was presented at ICAE2020, Dec. 1-Dec. 10, Bangkok/Virtual. This paper is a substantial extension of the short version of the conference paper.